EUROPEAN ORGANIZATION FOR NUCLEAR RESEARCH (CERN)

CERN-PH-EP/2011-084
2011/07/12

CMS-SUS-10-006

Search for supersymmetry in pp collisions at $\sqrt{s} = 7$ TeV in events with a single lepton, jets, and missing transverse momentum

The CMS Collaboration*

Abstract

Results are reported from a search for physics beyond the standard model in proton-proton collisions at a center-of-mass energy of 7 TeV, focusing on the signature with a single, isolated, high-transverse-momentum lepton (electron or muon), energetic jets, and large missing transverse momentum. The data sample comprises an integrated luminosity of 36 pb^{-1}, recorded by the CMS experiment at the LHC. The search is motivated by models of new physics, including supersymmetry. The observed event yields are consistent with standard model backgrounds predicted using control samples obtained from the data. The characteristics of the event sample are consistent with those expected for the production of $t\bar{t}$ and W+jets events. The results are interpreted in terms of limits on the parameter space for the constrained minimal supersymmetric extension of the standard model.

Submitted to the Journal of High Energy Physics

*See Appendix A for the list of collaboration members

1 Introduction

Searches for new physics at the TeV energy scale are motivated by several considerations, ranging from the strong astrophysical evidence for dark matter [1–4] to theoretical issues associated with explaining the observed particle masses and their hierarchy [5, 6]. In this paper, we report results from a search for new physics in proton-proton collisions at a center-of-mass energy of 7 TeV, focusing on the signature with a single isolated lepton (electron or muon), multiple energetic jets, and large missing momentum transverse to the beam direction ($\not\!\!E_{\mathrm{T}}$). The data sample was collected by the Compact Muon Solenoid (CMS) experiment during 2010 at the Large Hadron Collider (LHC) and corresponds to an integrated luminosity of 36 pb^{-1} [7].

The search signature arises naturally in several theoretical frameworks for new physics, among them supersymmetry (SUSY) [8–13]. SUSY models predict a spectrum of new particles with couplings identical to those of the standard model (SM), but with spins differing by half a unit with respect to their SM partners. In many models, a multiplicatively conserved quantum number, R parity, is introduced, constraining SUSY particles to be produced in pairs and SUSY particle decay chains to end with the lightest supersymmetric particle (LSP). In some scenarios, the LSP is a neutralino, a heavy, electrically neutral, weakly interacting particle with the characteristics required of a dark-matter candidate.

Searches at the Tevatron [14–16] and LEP [17–21] have found no evidence as yet for SUSY particles, demonstrating that, if supersymmetry exists, it is broken, with SUSY particle masses typically greater than 100–300 GeV. Recently, searches from the CMS [22–27] and ATLAS [28–32] experiments have extended the sensitivity to higher mass scales. In particular, ATLAS has reported [28] constraints on SUSY models from a search in the single-lepton channel, which is defined in a similar manner to this analysis.

At the LHC, relatively large cross sections for SUSY particle production (up to tens of pb) can arise from strong-interaction (QCD) processes leading to the production of gluino-gluino, squark-gluino, squark-squark, and squark-antisquark pairs. The search signature reflects the complex decay chains of the heavy, strongly coupled SUSY particles. The isolated lepton indicates a weak decay of a heavy particle, either a W boson or a new particle. Large missing momentum transverse to the beam direction can be carried by a neutrino or, in the case of new physics, by one or more heavy, weakly interacting particles, such as the LSP. Finally, multiple jets can arise from quarks and gluons produced in the decay chains. This signature arises in many SUSY models, including the constrained minimal supersymmetric extension to the standard model (CMSSM) [33, 34], which we use to interpret the results.

The SUSY signal is not characterized by any narrow peaks, but rather by broad distributions that extend to higher values of the kinematic variables than those of the SM backgrounds. These backgrounds arise primarily from the production of $\mathrm{t\bar{t}}$, W+jets, and QCD multijet events. It is therefore critical to determine the extent of the tails of the SM background distributions. We use methods that are primarily based on control samples in the data, sometimes in conjunction with certain reliable information from simulated event samples.

Two complementary methods are used to probe the event sample, one focusing mainly on jets and $\not\!\!E_{\mathrm{T}}$, and the other emphasizing the lepton transverse momentum (p_{T}) and $\not\!\!E_{\mathrm{T}}$. The first method uses two kinematic variables, H_{T} and $\not\!\!E_{\mathrm{T}}/\sqrt{H_{\mathrm{T}}}$, where H_{T} is the scalar sum of the jet p_{T} values for all jets above a certain threshold. The yields in three control regions are combined to provide a prediction for the total background in the signal region, without differentiating among the backgrounds. This method tests whether the behavior of the event sample with respect to jets and $\not\!\!E_{\mathrm{T}}$ is consistent with that expected from the SM.

The second method, which is ultimately used for the interpretation in terms of constraints on SUSY parameter space, exploits the relationship between the lepton p_T and the $\not{E}_T$ distributions. The dominant SM backgrounds are $t\bar{t}$ and $W(\ell\nu)$+jets events with a single, isolated, high-p_T lepton (ℓ = e or μ). In these processes, the lepton p_T and the $\not{E}_T$ distributions are closely related, because the lepton and neutrino are produced together in the two-body W decay. The observed lepton spectrum, with appropriate corrections, can therefore be used to predict the $\not{E}_T$ spectrum under the null (SM) hypothesis. In contrast, the distributions of lepton p_T and $\not{E}_T$ are very different in many SUSY models, where the presence of two LSPs effectively decouples the two distributions. In such models, the method is robust against potential signal contamination of the control regions. Smaller backgrounds from dilepton $t\bar{t}$ events (where both W bosons associated with the top quarks decay leptonically) feeding down to the single-lepton channel, and from $\tau \to \ell$ decays in both $t\bar{t}$ and W+jets events, are estimated from additional control samples, as is the QCD multijet background.

The two methods for probing the data provide a broader picture of the event sample than a single approach. Given the large range of potential signal models, the use of multiple methods for the background determination provides valuable information to ensure that the event sample is comprehensively understood.

The CMS detector, described in detail in Ref. [35], is a multipurpose apparatus designed to study high-p_T physics processes in proton-proton collisions, as well as a broad range of phenomena in heavy-ion collisions. The central element of CMS is a 3.8 T superconducting solenoid, 13 m in length and 6 m in diameter. Within the magnet are (in order of increasing radius from the beam pipe) the high-precision silicon-pixel and silicon-strip detectors for charged particle tracking; a lead tungstate crystal electromagnetic calorimeter for measurements of photons, electrons, and the electromagnetic component of jets; and a hadron calorimeter, constructed from scintillating tiles and brass absorbers, for jet-energy measurements. Beyond the magnet is the muon system, comprising drift-tube, cathode-strip, and resistive-plate detectors interleaved with steel absorbers. Each detector system comprises subsystems that cover the central (barrel) and forward (endcap) regions.

In describing the angular distribution of particles and the acceptance of the detector, we frequently make use of the pseudorapidity, $\eta = -\ln[\tan(\theta/2)]$, where the polar angle θ of the particle's momentum vector is measured with respect to the z axis of the CMS coordinate system. The z axis points along the direction of the counterclockwise rotating beam; the azimuthal angle ϕ is measured in a plane perpendicular to this axis. The separation between two momentum vectors in η-ϕ space is characterized by the quantity $\Delta R = \sqrt{(\Delta\eta)^2 + (\Delta\phi)^2}$, which is approximately invariant under Lorentz boosts along the z axis.

The paper is organized as follows. The event selection requirements are described in Section 2. Section 3 begins with a brief survey of the kinematic distributions, comparing the data with simulated Monte Carlo (MC) event samples. The methodologies for obtaining SM background estimates from control samples in the data are described, and the observed yields in the data are compared with these estimates. The systematic uncertainties are summarized in Section 4. Finally, the results, interpretation, and conclusions of the analysis are presented in Sections 5 and 6.

2 Event Samples and Preselection

This section describes the overall strategy of the analysis, the event samples used, and the preselection requirements. The composition of the event sample is determined largely by the

topological requirements of a single isolated, high-p_T lepton, either an electron or a muon, and at least four jets. The lepton-isolation requirement is critical for the rejection of QCD multijet processes, which have very large cross sections. While many lepton candidates are produced in the semileptonic decays of b and c hadrons, from π and K decays in flight, and from misidentification of hadrons, the vast majority of these are embedded in hadronic jets and are rejected using the lepton-isolation variable described below. The initially very large W+jets background (which is dominated by $W \to e\nu$ or $W \to \mu\nu$) is heavily suppressed by the four-jet requirement; $t\bar{t}$ then emerges as the largest contribution to the background in the sample of events with moderate to large values of missing transverse momentum (above approximately 150 GeV).

Because the analysis is part of a broad set of CMS topological SUSY searches involving $\not{E}_T$, we veto events containing a second isolated-lepton candidate. This procedure reduces the statistical overlap between the searches in different topologies, provides a clearer phenomenological interpretation of each search, and, in the single-lepton channel, suppresses SM backgrounds that produce two or more isolated leptons. Nevertheless, $t\bar{t}$ backgrounds with dileptons can still feed into the sample, and this contribution must be determined, particularly because the presence of two neutrinos can result in large values of $\not{E}_T$. The background involving $W \to \tau\nu$ decays, both from $t\bar{t}$ events and from direct W production, must also be determined.

The analysis procedures are designed by studying simulated event samples based on a variety of generators; in all cases except for certain SUSY scans discussed later, the detector simulation is performed using the GEANT4 package [36]. QCD samples are generated with the PYTHIA 6.4.22 [37] MC generator with tune Z2 [38]. The dominant background, $t\bar{t}$, is studied with a sample generated with MADGRAPH 4.4.12 [39]. The W+jets and Z+jets processes are simulated with both MADGRAPH and ALPGEN [40].

SUSY benchmark models are generated with PYTHIA. Two models, designated LM0 and LM1 [41], are frequently used in CMS because they have large cross sections and are accessible with small event samples. LM0 is described by the universal scalar mass parameter $m_0 = 200$ GeV, the universal gaugino mass parameter $m_{1/2} = 160$ GeV, the universal trilinear soft SUSY breaking parameter $A_0 = -400$ GeV, the ratio of the two Higgs-doublet vacuum expectation values $\tan\beta = 10$, and the sign of the Higgs mixing parameter $\mu > 0$. For LM1, the corresponding parameters are $m_0 = 60$ GeV, $m_{1/2} = 250$ GeV, $A_0 = 0$ GeV, $\tan\beta = 10$, and $\mu > 0$. The leading order cross sections for these models are 38.9 pb (LM0) and 4.9 pb (LM1); with K factors averaged over the contributing subprocesses, the next-to-leading order cross sections are approximately 54.9 pb (LM0) and 6.6 pb (LM1). These benchmark models are beyond the exclusion limits of the Tevatron and LEP searches referenced in Section 1, and have recently been excluded by LHC searches, e.g., Ref. [22]. They provide useful comparison points for searches in different channels. We also perform scans over CMSSM parameter space using a large number of Monte Carlo samples in which the simulation is performed using a CMS fast simulation package to reduce the time associated with the detector simulation.

The data samples used in the analysis are recorded using trigger paths that directly require the presence of a lepton above a minimum p_T threshold, sometimes in conjunction with additional jet energy. The basic muon trigger path is a simple, single-muon trigger requiring $p_T(\mu) > 11$ GeV. As the LHC luminosity increased above 2×10^{32} cm^{-2}s^{-1}, a trigger was implemented requiring both $p_T(\mu) > 5$ GeV and $H_T^{\text{trigger}} > 70$ GeV, where H_T^{trigger} is the scalar sum of the raw calorimeter jet E_T values measured at the trigger level. For electrons, a higher single-electron trigger threshold is required, $p_T(e) > 17$ GeV.

The offline preselection requirements are designed to be simple and robust. Events are required to have at least one good reconstructed primary vertex, at least four jets, and exactly one iso-

lated muon or exactly one isolated electron. (The jet and lepton selection criteria are specified below.) The primary vertex must satisfy a set of quality requirements, including $|z_{\mathrm{PV}}| < 24$ cm and $\rho_{\mathrm{PV}} < 2$ cm, where z_{PV} and ρ_{PV} are the longitudinal and transverse distances of the primary vertex with respect to the nominal CMS interaction point.

Jets and $\not\!\!E_{\mathrm{T}}$ are reconstructed using a particle-flow algorithm [42, 43], which combines information from all components of the detector. The $\not\!\!E_{\mathrm{T}}$ vector is defined as the negative of the vector sum of the transverse momenta of all the particles reconstructed and identified by the particle-flow algorithm. (The $\not\!\!E_{\mathrm{T}}$ quantity itself is the magnitude of the $\not\!\!E_{\mathrm{T}}$ vector.) The jet clustering is performed using the anti-k_{T} clustering algorithm [44] with a distance parameter of 0.5. Corrections based on simulation are applied to the raw jet energies to establish a relative uniform response across the detector in η and an absolute calibrated response in p_{T}. Additional jet-energy corrections are applied to the data to take into account residual differences between the jet-energy calibration in data and simulation. The performance of CMS jet reconstruction and the corrections are described in Refs. [45, 46]. Jet candidates are required to satisfy quality criteria that suppress noise and spurious energy deposits, and each event must contain at least four jets with $p_{\mathrm{T}} > 30$ GeV and $|\eta| < 2.4$.

In the muon channel, the preselection requires a single muon candidate [47] satisfying $p_{\mathrm{T}}(\mu) > 15$ GeV and $|\eta| < 2.1$. Several requirements are imposed on the elements that form the muon candidate. The reconstructed track must have at least 11 hits in the silicon tracker, with an impact parameter d_0 in the transverse plane with respect to the beam spot satisfying $d_0 < 0.02$ cm and an impact parameter d_z with respect to the primary vertex along the z (beam) direction satisfying $|d_z| < 1.0$ cm. To suppress background in which the muon originates from a semileptonic decay of a b or c quark in a jet, we require that it be spatially isolated from other energy in the event. A cone of size $\Delta R = 0.3$ is constructed around the muon direction in η-ϕ space. The muon isolation variable, $I = \sum_{\Delta R<0.3}(E_{\mathrm{T}} + p_{\mathrm{T}})$, is defined as the sum of the transverse energy E_{T} (as measured in the electromagnetic and hadron calorimeters) and the transverse momentum p_{T} (as measured in the silicon tracker) of all reconstructed objects within this cone, excluding the muon. This quantity is used to compute the isolation relative to the muon transverse momentum, which is required to satisfy $I/p_{\mathrm{T}}(\mu) < 0.1$. Finally, the muon must satisfy $\Delta R > 0.3$ with respect to all jets with $p_{\mathrm{T}} > 30$ GeV and $|\eta| < 2.4$.

For the electron channel, a single electron candidate [48] is required to satisfy $p_{\mathrm{T}} > 20$ GeV and $|\eta| < 2.4$, excluding the barrel-endcap overlap region $1.44 < |\eta| < 1.57$. The relative isolation variable, defined as in the muon case, must satisfy $I/p_{\mathrm{T}}(\mathrm{e}) < 0.07$ in the barrel region and $I/p_{\mathrm{T}}(\mathrm{e}) < 0.06$ in the endcaps, as well as a set of quality and photon-conversion rejection criteria. Events with two or more good lepton candidates are rejected, for the reasons discussed above.

3 Signal Regions and Background Determination

We next survey the properties of the event sample after imposing the preselection requirements described in the previous section, and after further requiring $\not\!\!E_{\mathrm{T}} > 25$ GeV. While this $\not\!\!E_{\mathrm{T}}$ requirement is far looser than that used in the final selection, it nevertheless suppresses much of the remaining QCD multijet background and brings the sample closer to the final composition dominated by $\mathrm{t\bar{t}}$ and W+jets events. The overall shapes of the observed distributions are found to be consistent with those expected for these backgrounds. We then proceed to apply methods, based on control samples in the data, that are designed to determine the SM contributions to the tails of the kinematic distributions in the signal regions.

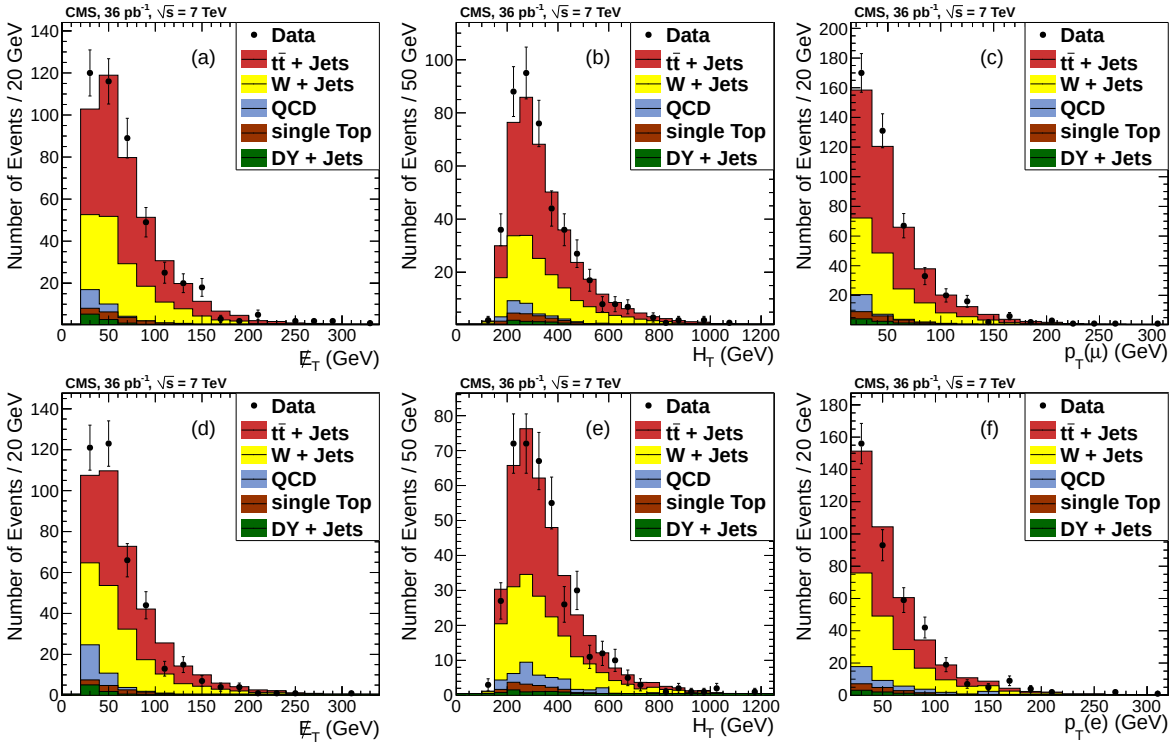

Figure 1: Comparison of distributions in data and simulated event samples for the muon channel: (a) $\not\!\!E_{\mathrm{T}}$, (b) H_{T}, and (c) lepton p_{T}; and for the electron channel (d) $\not\!\!E_{\mathrm{T}}$, (e) H_{T}, and (f) lepton p_{T}. The data are shown by points with error bars; the simulation is displayed as the histogram with the individual components stacked. The preselection and $\not\!\!E_{\mathrm{T}} > 25$ GeV requirements have been applied.

The quantity H_{T} is defined as the scalar sum of the transverse momenta of jets j with $p_{\mathrm{T}}^{j} > 20$ GeV and $|\eta| < 2.4$,

$$H_{\mathrm{T}} = \sum_{j} p_{\mathrm{T}}^{j}. \tag{1}$$

A simple requirement on the p_{T} of the highest p_{T} or the two highest p_{T} jets can also provide discrimination between signal and background, but such a requirement is more directly sensitive to the mass splittings in a new physics model than H_{T}. Thus, we prefer to use H_{T} to reduce the potential model dependence of the analysis.

After applying the preselection and $\not\!\!E_{\mathrm{T}} > 25$ GeV as a loose requirement, 444 (391) events are observed in data in the muon (electron) channel, compared with 395 (327) muon (electron) events in the simulated event samples. The estimate from simulation is based on summing the yields from $\mathrm{t\bar{t}}$, W+jets, Drell-Yan/Z+jets, QCD multijet, and single-top production. The contributions from $\mathrm{t\bar{t}}$ and W+jets account for about 90% of the predicted yield. The number of events obtained from simulation is not the basis for our background predictions, which rely primarily on control samples in the data. However, the approximate agreement between yields in data and simulation is a first indication that the analysis methods will be applied to a sample dominated by SM events.

Figure 1 shows the distributions from data and simulated event samples of three fundamental quantities in the muon and electron channels: $\not\!\!E_{\mathrm{T}}$, H_{T}, and lepton p_{T}. For the purpose of these comparisons, the normalization of the $\mathrm{t\bar{t}}$ sample is fixed by the integrated luminosity

and the next-to-leading-order (NLO) cross section, 157 pb, obtained using MCFM [49, 50]. The QCD multijet component is fixed by the PYTHIA-based simulation. Because of the $\not\!\!E_T > 25$ GeV requirement, the QCD yield is small and its uncertainty does not substantially affect the comparison. To allow for a better comparison of the shapes of the distributions, the W+jets normalization is adjusted so that the total event yields in data and simulation agree, resulting in an increase by ≈40% with respect to the inclusive next-to-next-to-leading order (NNLO) value, $\sigma(W(\ell\nu)) = 31.3$ nb (obtained using FEWZ [51] and summed over all three lepton flavors). A similar effect is observed in the CMS $t\bar{t}$ cross section measurement in the single-lepton channel, as discussed in Ref. [52]. This scaling is applied only for these illustrative plots and is not relevant to the procedures used to obtain the background contributions for the actual measurement.

The overall shapes of these and many other distributions are in qualitative agreement with the simulation. We have examined the p_T distributions of the four leading jets, the invariant mass distribution of the three leading jets, the lepton isolation distributions, the number of b-tagged jets, and the transverse mass of the lepton-$\not\!\!E_T$ system, which corresponds to the W boson in most SM background processes. We conclude that the cores of the observed distributions are dominated by $t\bar{t}$ and W+jets events.

Because the signal region involves the extreme tails of these distributions, which are difficult to simulate, the background predictions are based on control samples in the data rather than on simulated event samples. The following sections describe these methods, which further probe the detailed kinematic features of the event sample.

3.1 Background determination using H_T and $\not\!\!E_T/\sqrt{H_T}$

Two kinematic variables that discriminate between SM backgrounds and new physics models such as SUSY, are $\not\!\!E_T$ and H_T. Using a rescaled version of $\not\!\!E_T$ to minimize the correlation with H_T,

$$Y_{MET} \equiv \not\!\!E_T / \sqrt{H_T}, \tag{2}$$

where H_T is given by Eq. (1), we can construct a set of control regions in the two-dimensional kinematic space of (H_T, Y_{MET}) and use them to obtain a background estimate in the signal region. The quantity Y_{MET} can be interpreted as an approximate $\not\!\!E_T$ significance in that the denominator is proportional to the uncertainty on $\not\!\!E_T$ arising from jet mismeasurements [53].

The critical feature of these variables is that, due to the lack of significant correlation in the kinematic regions and event samples used in this analysis, their joint probability distribution is, to a good approximation, simply the product of the individual, one-dimensional distributions. These variables and a similar procedure were also used in the CMS opposite-sign dilepton SUSY search [25].

Table 1 defines "loose" and "tight" kinematic regions in the space of (H_T, Y_{MET}), with four sub-regions denoted by A, B, C, and D in each case. Regions A, B, and C have either low Y_{MET} or H_T or both, while region D, the signal region, has high values of both variables. Due to the very small correlation, the ratio of high-to-low Y_{MET} events is nearly independent of H_T, and the number of SM background events in region D can be estimated from $N(D)_{pred} = [N(C)/N(A)]N(B)$, where $N(i)$ denotes the number of events in region i. The tight selection was designed for SUSY models with small cross sections and higher masses, while the loose selection is sensitive to large cross sections and provides an additional handle for the comparison with the SM background prediction.

Table 1: Definitions of the regions A, B, C, and D with the loose and tight regions for the background estimation method using H_T and Y_{MET}.

Region	Loose selection		Tight selection	
	H_T (GeV)	Y_{MET} ($\sqrt{GeV}$)	H_T (GeV)	Y_{MET} ($\sqrt{GeV}$)
A	$300 < H_T < 350$	$2.5 < Y_{MET} < 4.5$	$300 < H_T < 650$	$2.5 < Y_{MET} < 5.5$
B	$H_T > 400$	$2.5 < Y_{MET} < 4.5$	$H_T > 650$	$2.5 < Y_{MET} < 5.5$
C	$300 < H_T < 350$	$Y_{MET} > 4.5$	$300 < H_T < 650$	$Y_{MET} > 5.5$
D	$H_T > 400$	$Y_{MET} > 4.5$	$H_T > 650$	$Y_{MET} > 5.5$

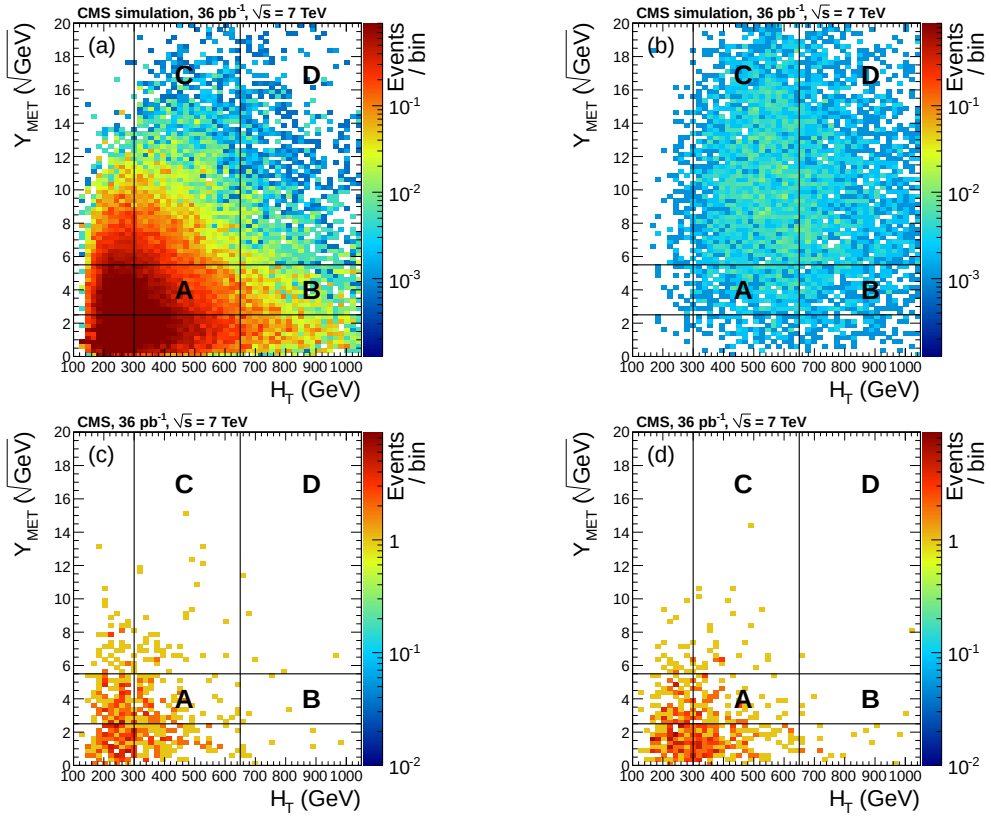

Figure 2: Distributions of H_T vs. Y_{MET} for (a) the simulated total SM background (muon channel), (b) SUSY LM1 (muon channel), (c) data in the muon channel, and (d) data in the electron channel. The control regions ABC and the signal region D are shown for the tight selection.

Figure 2 shows the two-dimensional distributions of H_T vs. Y_{MET} for the simulated signal and background samples, as well as for the data. For the signal samples, we have used the LM1 SUSY benchmark model, normalized to the integrated luminosity of the data sample using the NLO cross section given in Section 2. Events from this model are distributed at significantly higher values of H_T and Y_{MET} than those for the $t\bar{t}$ and W+jets backgrounds, reflecting the higher mass scales of the particles produced in SUSY events.

The Y_{MET} distributions for events satisfying the preselection requirements and $H_T > 300$ GeV (the lower H_T requirement on regions A and B) are shown in Fig. 3 for the muon and electron channels. The shape of the Y_{MET} distribution observed in the data agrees well with that predicted from the combined simulated event samples. In the electron channel an excess is

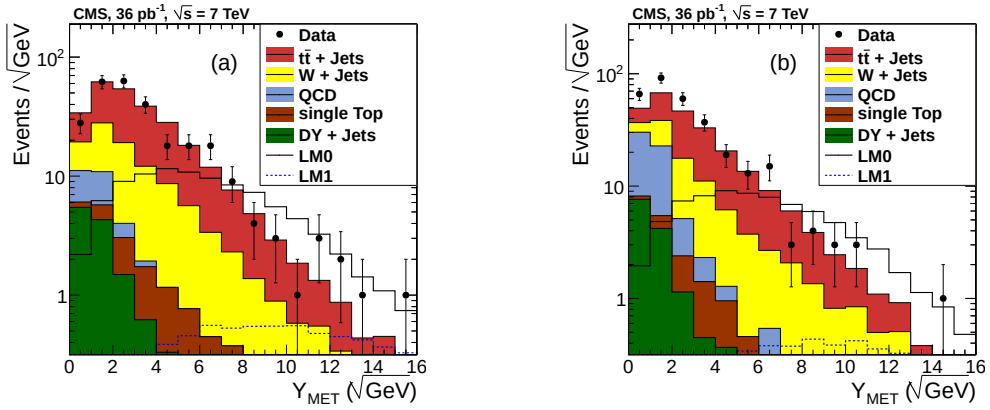

Figure 3: Data and simulated (MC) distributions of Y_{MET} for (a) the muon channel and (b) the electron channel after the preselection and $H_{\text{T}} > 300$ GeV requirements. The simulated SM distributions are stacked; the distributions for the SUSY LM0 and LM1 benchmark models are overlaid.

Table 2: Data and simulated (MC) event samples: predicted and observed yields for the H_{T} vs. Y_{MET} background estimation method. Tests of the method based on simulated event samples are included for comparison, but the actual background prediction is based on applying the procedure to the data. The predicted yields, $N(D)_{\text{pred}}$, in the signal region computed using the yields observed in regions A, B, and C, as described in the text; these predictions are consistent with the observed yields in region D. The uncertainties shown are statistical only for simulation and statistical and systematic for the prediction in data. The systematic uncertainties on $N(D)_{\text{pred}}$ for data are discussed in Section 4.

sample	$N(A)$	$N(B)$	$N(C)$	$N(D)$	$N(D)_{\text{pred}}$
			Loose selection		
μ channel: total SM MC	25.1 ± 0.6	37.1 ± 0.7	19.3 ± 0.5	30.6 ± 0.6	28.5 ± 1.1
μ channel: data	30	35	25	30	$29.2 \pm 9.3 \pm 4.1$
e channel: total SM MC	20.0 ± 0.5	31.5 ± 0.9	14.6 ± 0.5	23.6 ± 0.5	22.9 ± 1.2
e channel: data	19	33	19	17	$33.0 \pm 12.2 \pm 5.1$
			Tight selection		
μ channel: total SM MC	93.1 ± 1.1	8.7 ± 0.4	37.6 ± 0.7	3.4 ± 0.2	3.5 ± 0.2
μ channel: data	98	4	41	5	$1.7 \pm 0.9 \pm 0.3$
e channel: total SM MC	76.8 ± 1.5	6.5 ± 0.3	29.5 ± 0.7	2.9 ± 0.2	2.5 ± 0.1
e channel: data	80	4	30	2	$1.5 \pm 0.8 \pm 0.3$

observed in the low Y_{MET} bins — a region where simulation predicts a contribution of QCD multijet events to the total background of about one third (compared to Fig. 1 no explicit $\not\!\!E_{\text{T}}$ cut is applied in this selection). The number of QCD multijet events in each of the four $ABCD$ regions, however, was measured from data and found to be small.

Table 2 shows the event yields in the data and in the simulated background samples in the four regions, together with the predicted background level based on this method. In both lepton channels, and for both the loose and tight selections, the predictions are statistically consistent with the observed yields in the signal region. Section 4 discusses the sources of systematic uncertainty, including small correlation effects and a potential bias from the small QCD multijet background.

In summary, we observe $N_{obs}(\mu) = 5$ and $N_{obs}(e) = 2$ events in the signal region (D) after applying the tight selection requirements in the muon and electron channels. The predicted yields, based on the control regions in the H_T vs. $\not\!\!E_{MET}$ kinematic space, are $N(\mu) = 1.7 \pm 0.9\,(\text{stat.}) \pm 0.3\,(\text{syst.})$ and $N(e) = 1.5 \pm 0.8\,(\text{stat.}) \pm 0.3\,(\text{syst.})$, which are statistically compatible with the observed yields. For the tight selection the predicted yields for the SUSY benchmark models described in Section 2 are $22.5 \pm 0.7\,(\text{stat.})$ events for LM0 and $4.6 \pm 0.1\,(\text{stat.})$ events for LM1, with the yields divided approximately equally between the muon and electron channels.

3.2 Background determination using the $\not\!\!E_T$ and lepton p_T distributions

This section describes the lepton-spectrum method [54] for determining the shape of the $\not\!\!E_T$ distribution from $t\bar{t}$ and W+jets backgrounds with a single isolated lepton. These processes account for about 70% of the total SM contribution to the signal region, once the final selection requirements are applied. We also describe methods using control samples in data to measure most of the remaining background components. These arise mainly from (1) the feed-down of $t\bar{t}$ dilepton events (≈15%) and (2) either $t\bar{t}$ or W+jets events with $\tau \to (\mu, e)$ decays (≈15%). Although the background from QCD multijet events is very small, we nevertheless measure this component using control samples in the data, because the uncertainties on the simulated QCD event samples are difficult to quantify. We rely on simulated event samples for the determination of two backgrounds, single-top production and Z+jets, whose contributions are estimated to be below one event in total.

Two signal regions, loose and tight, are defined. The loose selection consists of the preselection requirements (with, however, $p_T(\ell) > 20$ GeV for both e and μ for consistency), together with the requirement $\not\!\!E_T > 150$ GeV. For the tight selection, we require $\not\!\!E_T > 250$ GeV and $H_T > 500$ GeV, in addition to the loose selection cuts. The tight selection is motivated by the fact that for models with higher mass scales, the $\not\!\!E_T$ and H_T distributions are shifted upward, but the production cross sections fall rapidly.

We distinguish between two forms of $\not\!\!E_T$, genuine and artificial, that contribute to the reconstructed $\not\!\!E_T$ distribution. With the selection requirements used here, the dominant source of $\not\!\!E_T$ arises from the high-momentum neutrinos produced in W decay and hence is genuine. Artificial $\not\!\!E_T$ from jet mismeasurement is a much smaller effect but is not negligible and must be taken into account.

The physical foundation of the lepton-spectrum method is that, when the lepton and neutrino are produced together in two-body W decay (either in $t\bar{t}$ or in W+jets events) the lepton spectrum is directly related to the $\not\!\!E_T$ spectrum. With suitable corrections, discussed below, the lepton spectrum can therefore be used to predict the $\not\!\!E_T$ spectrum. In contrast, the $\not\!\!E_T$ distribution in most SUSY models is dominated by the presence of two LSPs. The $\not\!\!E_T$ distribution for such models extends to far higher values than the lepton spectrum. These points are illustrated in Fig. 4, which shows the relationship between lepton-p_T and $\not\!\!E_T$ distributions in the laboratory frame for two simulated event samples: (a) the predicted SM mixture of $t\bar{t}$ and W+jets events and (b) the SUSY LM1 benchmark model. As we will demonstrate, the lepton-spectrum method provides a robust background prediction in the high $\not\!\!E_T$ region, even in the presence of a large SUSY signal, because leptons in SUSY events typically have much lower momenta than the LSPs.

To use the lepton spectrum to predict the $\not\!\!E_T$ spectrum in single-lepton SM background processes, three issues must be addressed: (1) the effect of W-boson polarization in both $t\bar{t}$ and W+jets events, (2) the effect of the applied lepton p_T threshold, and (3) the effect of the dif-

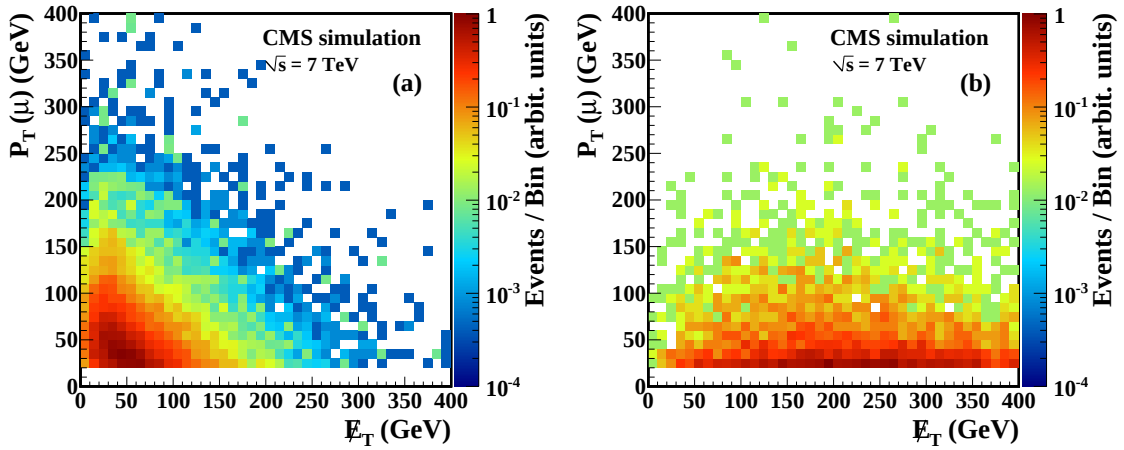

Figure 4: Distributions of muon p_T vs. $\not{E}_T$ in the μ channel for (a) simulated $t\bar{t}$ and W+jets events and (b) the LM1 SUSY benchmark model. In $t\bar{t}$ and W+jets events, the lepton p_T and $\not{E}_T$ in a given event are anticorrelated, but their distributions are very similar overall. In LM1, which is typical of many SUSY models, the $\not{E}_T$ distribution is much harder than the lepton spectrum, since it is dominated by the production of two LSPs.

ference between the experimental resolutions on the measurements of lepton p_T and $\not{E}_T$. We consider the polarization issues first. In each of these background processes, the leptons are produced in two-body W-boson decays, so that the momenta of the lepton and the neutrino are equal and opposite in the W rest frame, with angular distributions governed by the W polarization. On an event-by-event basis, these momenta undergo identically the same sequence of Lorentz transformations from the W rest frame to the lab frame, so in this sense the lepton spectrum automatically incorporates the effects of the t-quark and W-boson p_T distributions. While the lepton and neutrino momenta are anticorrelated in the laboratory frame on an event-by-event basis, the integrated distributions are very similar. If the angular distributions in the W rest frame were forward-backward symmetric, the lab-frame $\not{E}_T$ and lepton-p_T distributions would be identical. However, the helicity ± 1 polarization states of the W boson produce forward-backward asymmetries that can shift the lepton-p_T spectrum with respect to the $\not{E}_T$ spectrum.

We first consider $t\bar{t}$ production, which is the largest background. In the decay of a top quark, $t \to bW^+$, the angular distribution of the (positively) charged lepton in the W^+ rest frame can be written

$$\frac{dN}{d\cos\theta_\ell^*} = f_{+1}\frac{3}{8}(1+\cos\theta_\ell^*)^2 + f_{-1}\frac{3}{8}(1-\cos\theta_\ell^*)^2 + f_0\frac{3}{4}\sin^2\theta_\ell^*, \tag{3}$$

where f_{+1}, f_{-1}, and f_0 denote the polarization fractions associated with the W-boson helicities $+1$, -1, and 0, respectively. The angle θ_ℓ^* is the polar angle of the charged lepton in the W^+ rest frame, measured with respect to a z-axis that is collinear with the momentum direction of the W^+ in the top-quark rest frame. (In this expression, the azimuthal angle has been integrated over, removing the interference terms between different helicity amplitudes.) The polarization fractions thus determine the angular distribution of the lepton in the W rest frame and, together with the Lorentz boosts, control the p_T distributions of the lepton and the neutrino in the laboratory frame.

The W polarization fractions in top-quark decay have been calculated [55] with QCD correc-

tions to NNLO, and the polarization is predominantly longitudinal. For $t \to bW^+$ these fractions are $f_0 = 0.687 \pm 0.005$, $f_{-1} = 0.311 \pm 0.005$, and $f_{+1} = 0.0017 \pm 0.0001$. The very small value of f_{+1} is explained by the fact that, since $m_b/m_W \ll 1$, the b quark is highly relativistic and is in a nearly pure helicity $\lambda = -1/2$ state. Conservation of angular momentum along the t-quark decay axis then forbids $\lambda = +1$ for the W boson. For the case of $\bar{t}$ rather than t decay, the W-boson helicity fractions are swapped between the $\lambda = \pm 1$ states, but the actual angular distribution of the lepton is identical, because of the corresponding reversal of the helicity state for the outgoing lepton, which has opposite charge. These precise calculations reduce the uncertainties associated with the W polarization in $t\bar{t}$ events to a low level. The theoretical values are consistent with measurements from CDF, which obtained [56] $f_0 = 0.88 \pm 0.11 \pm 0.06$ and $f_{+1} = -0.15 \pm 0.07 \pm 0.06$, expressed for the W^+ polarizations.

If the W polarization were entirely longitudinal ($\lambda = 0$), the angular distribution in the W rest frame would be forward-backward symmetric, and the momentum spectra of the lepton and neutrino would be identical in the laboratory frame. The effect of the substantial $\lambda = -1$ helicity component in W^+ decay is to give the lepton a preferred direction that is opposite to the W^+ momentum direction in the t rest frame. The asymmetry produces a somewhat softer lepton spectrum than the $\not\!\!E_T$ spectrum, for both t and $\bar{t}$ decays. The lepton spectrum therefore slightly underpredicts the high-$\not\!\!E_T$ tail in $t\bar{t}$ events, but the effect is well understood and is included as a correction.

The W polarization in W+jets events exhibits a more complex behavior than that in $t\bar{t}$ production. CMS has reported first measurements of these effects [57], which are consistent with ALPGEN and MADGRAPH simulations predicting that the W^+ and W^- bosons are both predominantly left-handed in W+jets events at high p_T. An NLO QCD calculation [58] has demonstrated that the predicted polarization fractions are stable with respect to QCD corrections. In contrast to $t\bar{t}$ events, where only two of the W polarization states are effectively present, all three W polarization states have significant amplitudes in W+jets events. In addition, *both* of the W^+ and W^-decay polarization fractions for $\lambda = -1$ are in the range 55–70% and increase gradually with $p_T(W)$. Because the $W^\pm$ daughter leptons have opposite helicities, this leads to *opposite* asymmetries for the lepton angular distributions. The cancellation in the asymmetries is not perfect, however, mainly because the W^+ cross section in pp collisions is substantially higher than that for W^-production. With the $\not\!\!E_T$ and lepton p_T requirements applied in the analysis, the relevant W bosons have $p_T(W) > 150$ GeV. The systematic uncertainties associated with these effects are discussed in Section 4.

The relationship between the lepton p_T spectrum and the $\not\!\!E_T$ distribution is also affected by the threshold ($p_T > 20$ GeV) applied to the leptons. Because of the anticorrelation between the lepton p_T and the $\not\!\!E_T$, the threshold requirement removes SM background events at high $\not\!\!E_T$ but not the events with high-p_T leptons that are used to predict this part of the $\not\!\!E_T$ spectrum. For the $t\bar{t}$ background, this effect partially compensates for the bias from the W polarization. For W+jets events, in contrast, the polarization effects for W^+ and W^- approximately cancel, but the lepton p_T threshold shifts the predicted yield upward. The key point is that the effects of both the polarization and the lepton p_T threshold can be reliably determined.

Finally, the resolution on the reconstructed $\not\!\!E_T$ is poorer than that for the lepton p_T, so the $\not\!\!E_T$ spectrum will be somewhat broadened with respect to the prediction from the lepton spectrum. We measure $\not\!\!E_T$ resolution functions (templates) in the data using QCD multijet events, and use them to smear the measured lepton momenta. The templates are created for events with ≥ 4 jets and are characterized by the H_T range of the events. Because the templates are taken from data, they include not only the intrinsic detector resolutions, but also the effects of cracks and

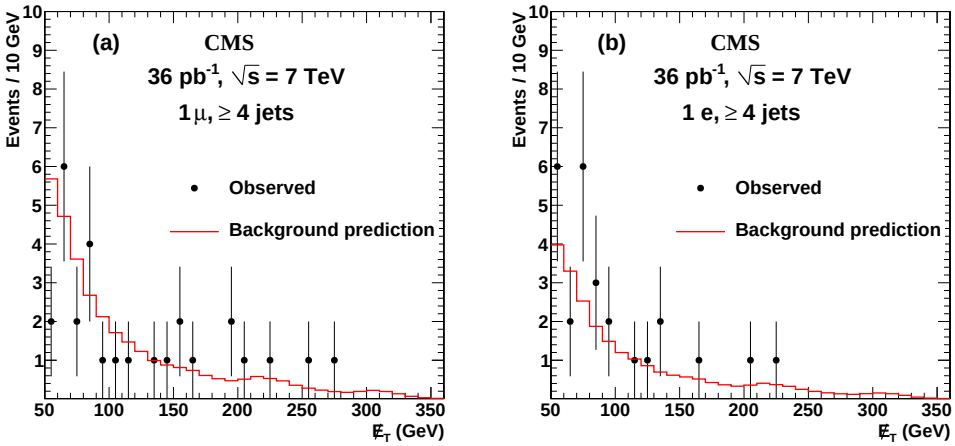

Figure 5: Measured vs. predicted $\not\!\!E_{\mathrm{T}}$ distributions in (a) muon and (b) electron channels, with tight selections applied. The data are shown as points with error bars, while the prediction from the resolutions-smeared lepton spectrum is shown as the histogram. The predicted single-lepton SM background yield for $\not\!\!E_{\mathrm{T}} > 250$ GeV is obtained from these curves, after applying a correction factor described in the text.

acceptance. The overall effect of the smearing is modest, changing the background prediction by 5–15%, depending on the $\not\!\!E_{\mathrm{T}}$ threshold applied.

The background predictions based on control samples in data require correction factors to account for a specific set of effects. For the single-lepton backgrounds, the effects of the W polarization, the lepton p_{T} threshold for the signal region, and the $\not\!\!E_{\mathrm{T}}$ energy scale are to produce understood shifts in the $\not\!\!E_{\mathrm{T}}$ spectrum relative to the lepton spectrum. The correction factors also account for a small contamination of the single-lepton control sample from dilepton and single-τ events with high p_{T} leptons, $\approx$2% for the tight selection. Overall, the lepton p_{T} spectra from these processes are much softer than the corresponding $\not\!\!E_{\mathrm{T}}$ distributions, and the background predictions must be obtained from separate control samples.

To account for these effects, the raw predicted yields are multiplied by correction factors, obtained from simulated event samples. The non-single-lepton backgrounds themselves are estimated from independent methods described below. For the tight selection the correction factors for the single-lepton background are near unity: 0.88 ± 0.07 for the muon channel and 0.89 ± 0.08 for the electron channel. In the loose selection, the factors are 0.62 ± 0.02 (muons) and 0.70 ± 0.02 (electrons). The uncertainties on the correction factors quoted here are statistical only. Systematic uncertainies are discussed in the following section.

Figure 5 shows the $\not\!\!E_{\mathrm{T}}$ distributions for the data in the muon and electron channels, with all of the tight selection requirements applied, except that on $\not\!\!E_{\mathrm{T}}$ itself. The predicted $\not\!\!E_{\mathrm{T}}$ distribution is obtained by applying the $\not\!\!E_{\mathrm{T}}$-smearing procedure, as described above, to the raw single-muon p_{T} spectrum. The predicted single-lepton background is in good agreement with the observed $\not\!\!E_{\mathrm{T}}$ spectra. The background predictions shown in Fig. 5 do not include the smaller contributions from non-single-lepton sources.

Tables 3 and 4 list the observed yields and the predicted SM background contributions for the loose and tight selection requirements. The event yields observed in the data are largely accounted for by the direct single-lepton backgrounds. As we have noted, however, the lepton-

Table 3: Loose selection: predicted and observed yields in the signal region (pre-selection, $\not\!\!E_T > 150$ GeV). The quoted uncertainties are statistical and systematic. All background contributions are determined from control samples in the data, except for the single-top and Z+jets contributions, which are obtained from simulated event samples.

Sample	$\ell = \mu$	$\ell = e$
Predicted SM 1 ℓ	$11.1 \pm 2.8 \pm 3.0$	$8.8 \pm 2.9 \pm 2.4$
Predicted SM dilepton	$1.0 \pm 0.6 \pm 0.1$	$0.8 \pm 0.5 \pm 0.03$
Predicted single τ	$2.1 \pm 0.6 \pm 0.2$	$2.2 \pm 0.5 \pm 0.3$
Predicted QCD background	$0.18 \pm 0.13 \pm 0.09$	$0.0^{+0.38}_{-0.0} \pm 0.19$
Predicted single top, Z+jets	$0.4 \pm 0.1 \pm 0.2$	$0.4 \pm 0.1 \pm 0.2$
Total predicted SM	$14.8 \pm 2.9 \pm 3.0$	$12.2 \pm 3.0 \pm 2.4$
Observed signal region	16	13

Table 4: Tight selection: predicted and observed yields in the signal region (pre-selection, $\not\!\!E_T > 250$ GeV, $H_T > 500$ GeV). The quoted uncertainties are statistical and systematic. All background contributions are determined from control samples in the data, except for the single-top and Z+jets contributions, which are obtained from simulated event samples.

Sample	$\ell = \mu$	$\ell = e$
Predicted SM 1 ℓ	$1.5 \pm 1.1 \pm 0.7$	$1.1 \pm 0.8 \pm 0.5$
Predicted SM dilepton	$0.0^{+0.3+0.23}_{-0.0-0.0}$	$0.0^{+0.4+0.14}_{-0.0-0.0}$
Predicted single τ	$0.16 \pm 0.10 \pm 0.20$	$0.27 \pm 0.20 \pm 0.20$
Predicted QCD background	$0.09^{+0.12}_{-0.09} \pm 0.04$	$0.0^{+0.16}_{-0.0} \pm 0.08$
Predicted single top, Z+jets	$0.05^{+0.05}_{-0.04} \pm 0.05$	$0.01 \pm 0.003 \pm 0.01$
Total predicted SM	$1.8 \pm 1.1 \pm 0.8$	$1.4 \pm 0.9 \pm 0.5$
Observed signal region	2	0

spectrum method does not comprehensively predict all of the backgrounds to the single-lepton sample, and non-negligible backgrounds arise from other sources, including several categories of dilepton events, events with $\tau \to \ell$ decays (either from $t\bar{t}$ or W+jets events), and QCD multijet processes. These contributions are also estimated using control samples in the data, as discussed below. The background from single-top production and Drell-Yan/Z+jets is very small for the loose selection and is negligible for the tight selection. These contributions are estimated from Monte Carlo samples, with systematic uncertainties taken to be 50% (100%) for the loose (tight) selection. Because of their small absolute size, these uncertainties have a negligible effect on the total background uncertainty.

The dilepton background (including the τ as one of the leptons) can be divided into four contributions: (1) 2ℓ with one ignored lepton, (2) 2ℓ with one lost lepton, (3) $\ell + \tau$ with $\tau \to$ hadrons, and (4) $\ell + \tau$ with $\tau \to$ lepton. An ignored lepton is one that is reconstructed but fails either the lepton identification requirements or the p_T threshold requirement. A lost lepton is one that is either not reconstructed or is out of the detector acceptance. Events from processes (1) and (3) account for most of the dilepton background. All of the estimates of the dilepton feed-down backgrounds begin with control samples of reconstructed dilepton events in the ee, eμ, and $\mu\mu$ channels. The $\not\!\!E_T$ distributions in these control samples in data, when suitably modified to reflect the loss of a lepton or the presence of a leptonic or hadronic τ decay, provide an accurate description of the shape of the $\not\!\!E_T$ distribution of the background. Simulated event samples are used to determine, for the four processes described above, the ratio $r_i = N^i_{\text{feed}}/N_{\text{control}}$ of the

number of events feeding down to the single-lepton channel to the number of events observed in the control sample. This procedure effectively normalizes all such feed-down contributions to the control samples in data. In all cases, care is required to ensure that the control sample is not contaminated by QCD background. Estimates for the $\tau \to \ell$ single-lepton backgrounds from $t\bar{t}$ and W+jets processes are based on a similar procedure as that used for the dilepton backgrounds, but in this case the single-lepton sample itself is used as the control sample.

We define correction factors for the dilepton and single-τ background predictions. In the loose selection, these corrections range from 0.86 to 0.94, with ≈10% uncertainty. For the tight selection, the correction factors are typically ~ 0.5, with a large (≈75%) systematic uncertainty. This correction has almost no effect on the final result, because the background from these sources is small compared to the single-e and single-μ backgrounds (see Tables 3 and 4).

Background from QCD multijet events is suppressed to a level well below one event in both the loose and tight selections. To estimate the QCD background, we use the two-dimensional distribution of $\not\!\!E_{\mathrm{T}}$ and the relative lepton isolation, $I/p_{\mathrm{T}}(\ell)$ (Section 2), which are essentially uncorrelated. Using a QCD-dominated sample with $\not\!\!E_{\mathrm{T}} < 25$ GeV, we measure the ratio of the number of leptons passing the isolation requirement ($I/p_{\mathrm{T}}(\ell) < 0.1$) to the number in an isolation sideband ($0.2 < I/p_{\mathrm{T}}(\ell) < 0.5$). Events that pass the $\not\!\!E_{\mathrm{T}}$ requirements for the signal region, but are in the isolation sideband, are then scaled by this measured ratio.

The precision of the QCD background prediction is limited by the small number of sideband leptons in the high-$\not\!\!E_{\mathrm{T}}$ region. Two such muon events are found with $\not\!\!E_{\mathrm{T}} > 150$ GeV, one of which also passes the $\not\!\!E_{\mathrm{T}} > 250$ GeV requirement, while there are no electron events. This procedure tends to overestimate the QCD background, because events from electroweak and $t\bar{t}$ processes can contaminate the high-$\not\!\!E_{\mathrm{T}}$ isolation sideband and the isolated, low-$\not\!\!E_{\mathrm{T}}$ sample. In addition, for the tight selection the measurement is performed using a loosened H_{T} requirement of 120 GeV for muons and 300 GeV for electrons, since the isolation sideband is sparsely populated. Despite these potential overestimates, the background predictions and their uncertainties, listed in Tables 3 and 4, are small, well below one event.

Although very few QCD background events contribute to the signal region at high $\not\!\!E_{\mathrm{T}}$, such events can affect the control region used to estimate the single-lepton background from $t\bar{t}$ and W+jets events. That control sample is selected without a $\not\!\!E_{\mathrm{T}}$ requirement. In fact, requiring a minimum value of $\not\!\!E_{\mathrm{T}}$, say $\not\!\!E_{\mathrm{T}} > 25$ GeV, would tend to remove events with high-p_{T} leptons, which are precisely those used to predict the high-$\not\!\!E_{\mathrm{T}}$ tail. The QCD contamination in the muon sample is very small, but there is significant contamination from QCD in the electron sample at low $\not\!\!E_{\mathrm{T}}$. We have therefore used only the p_{T} spectrum from the muon control sample to predict the rates for both the electron and muon signal regions. The scaling from the muon to the electron samples is obtained by fitting their ratio in the data over the range $60 < \not\!\!E_{\mathrm{T}} < 140$ GeV, with systematic uncertainties evaluated by varying the fit range. The resulting correction factor, $N(\mathrm{e})/N(\mu) = 0.70 \pm 0.15$, is consistent with the value obtained using simulated event samples.

In summary, the background yields listed in Tables 3 and 4 are consistent with the total background predicted in each selection, for both the electron and muon channels. In the loose selection, 16 muon events are observed in data compared with $14.8 \pm 2.9 \pm 3.0$ predicted, while 13 electron events are observed in data compared with $12.2 \pm 3.0 \pm 2.4$ predicted. In the tight selection, 2 muon events are observed in data compared with $1.8 \pm 1.1 \pm 0.8$ predicted, while 0 electron events are observed compared with $1.4 \pm 0.9 \pm 0.5$ predicted. The interpretation of these results in terms of SUSY models is discussed in Section 5.

4 Systematic Uncertainties

This section discusses the systematic uncertainties associated with the H_T vs. Y_{MET} and the lepton-spectrum methods. The uncertainties fall into two main categories: the uncertainties on the background estimates and the uncertainties on the overall acceptance and efficiency factors that are used to convert the observed yields into upper limits on SUSY cross sections.

The H_T vs. Y_{MET} method predicts the background yield in the signal region (D) as a function of the yields in the control regions A, B, and C. The systematic uncertainty arises from the possibility of a non-zero correlation between the kinematic variables and can be expressed in terms of small departures of the quantity $\kappa \equiv N(A)N(D)/N(B)N(C)$ from unity. Monte Carlo simulation predicts values of κ close to unity for $t\bar{t}$, W+jets, and single-top production, as well as for the sum of all backgrounds. As an additional check, this behavior of κ has also been verified for the three-jet samples, which are not used in the analysis.

We have evaluated the effect on κ from an extensive list of uncertainties. Reconstruction-related uncertainties include the jet (and $\not\!\!E_T$) energy scales, the jet-energy resolution, the amount of energy in the calorimeter not clustered into jets, the jet reconstruction efficiency, the lepton-p_T scale, and the p_T dependence of the efficiency. Physics-related uncertainties under consideration were related to the background composition ($t\bar{t}$ vs. W+jets), to the amount of QCD background subtracted from each control region, and to the parton distribution functions. The small deviation of the central value of κ from unity predicted by the simulation has been added as an additional uncertainty. These sources of systematic uncertainties are taken to be uncorrelated and the contributions are added in quadrature. For the loose selection, the total systematic uncertainties affecting the background prediction in the muon and electron channels are 14% and 16%, respectively. The corresponding numbers for the tight selection are 16% (μ) and 21% (e).

The systematic uncertainties on the lepton-spectrum background predictions are substantially larger, and they increase from the loose to the tight selection. The dominant uncertainty is associated with the jet and $\not\!\!E_T$ energy scale [46]. If this scale shifts relative to the lepton p_T scale, the predicted number of events above the $\not\!\!E_T$ threshold for the signal region will change. The 5% uncertainty on this scale propagates to a 22% uncertainty for the loose selection and a 37% uncertainty for the tight selection.

The precision with which the lepton spectrum prediction matches the $\not\!\!E_T$ spectrum is determined by a set of related effects, as described in Section 3.2. The helicity fractions for W bosons produced in $t\bar{t}$ events are predicted in the SM to high precision; when these uncertainties are propagated through the analysis, the effect on the background prediction is negligible. As a test, we have varied the polarization factors through a range that is about ten times the theoretical uncertainties quoted in Ref. [55]. This leads to only a 2% effect for the loose selection and a 4% effect for the tight selection. We have also varied the t-quark p_T spectrum to study the effect of the boost on any differences arising from the polarizations. This variation is constrained by the agreement between data and simulation for the W-boson p_T spectrum, and leads to 5% (loose) and 7% (tight) uncertainties on the background yield. In addition, we vary the $t\bar{t}$ cross section by $\pm$30% and the W+jets cross section by $\pm$50% and measure the effect on the background prediction in simulated event samples (12% for loose, 16% for tight selection).

To account for the W polarization uncertainties, we have chosen three variations of the polarization fractions: (1) 100% variation on $f_{-1} - f_{+1}$, for both W^+ and W^-together (this is equivalent to an approximately 30% variation of the individual polarization fractions); (2) 10% variation of f_{-1} and f_{+1}, with constant sum, for the W^+ polarization, holding the W^-polarization fixed, and vice-versa; and (3) 100% variation of the longitudinal polarization fraction, f_0, for both W^+

and W^-. Each variation is applied in the same manner in three bins of $p_T(W)$: 50–100 GeV, 100–300 GeV, and > 300 GeV. We do not vary the polarization of events with $p_T(W) < 50$ GeV since these have a negligible contribution to the selected event sample. The sum of all three variations in quadrature yields a 7% systematic uncertainty for the loose selection and a 14% uncertainty for the tight selection.

The systematic uncertainty arising from the possible incorrect modeling of the p_T dependence of the lepton reconstruction and identification efficiency is estimated to be ≈4%. The effect of a potential mismodeling of jet reconstruction efficiencies is found to be negligible. The total systematic uncertainties on the lepton-spectrum method for predicting the single-lepton background is 27% for the loose selection and 44% for the tight selection. These do not include the uncertainties on the separate estimates for the dilepton and τ backgrounds based on control samples. These additional predictions are assigned a systematic uncertainty based on tests with simulated samples, including both the statistical uncertainty due to finite simulated event samples and any observed shift with respect to the true values.

The effect of the $\not\!\!E_T$ resolution (smearing) in simulated $t\bar{t}$ events (using simulated QCD $\not\!\!E_T$ templates) is to increase the background prediction by about 10% for the loose selection. The smearing from the data has been seen to increase the background prediction slightly more, by about 15%. We have increased the size of the template binning in H_T by factors of two and five and recomputed the resolution smearing in each case. The effects are negligible, demonstrating that the prediction is insensitive to the details of the templates.

To translate from the observed event yields to cross section limits, we must incorporate the effects of the signal efficiencies and acceptance. These quantities are taken from the simulated event samples, with cross-checks performed using the data as a validation. The uncertainties include those on the modeling in simulation of the lepton trigger and identification efficiencies (5%), on the jet and $\not\!\!E_T$ energy scales (17% in the lepton-spectrum method), on the possible variation of parton density functions (negligible), and on the luminosity (4%). The total systematic uncertainty on the efficiency and acceptance is 20%.

5 Results and Interpretation

Both of the methods used to determine the SM background predict yields that are compatible with the observed number of events. In the absence of a signal, we proceed to set exclusion limits on SUSY parameter space.

The potential signal contamination of the control samples in the data is model dependent and must be assessed separately for each signal-model hypothesis. We have performed a scan over CMSSM model points and have determined the number of such events that enter the control regions of our measurements. For the lepton-spectrum method, the contamination is small, 0.05 events on average. However, the method using control regions in the H_T vs. Y_{MET} plane suffers a much greater contamination of the control regions, especially for models with large cross sections. For the purpose of setting limits on the CMSSM, we have therefore used the values obtained from the lepton-spectrum method.

Combining the yields in the lepton-spectrum method from the e and μ channels, we observe 29 events in the loose selection and 2 events in the tight selection. The predicted SM background is 27.0 ± 7.0 events and 3.2 ± 2.3 events for the loose and tight selections, respectively. (Because the muon spectrum is used as a control sample for obtaining the single-lepton background in both the e and μ channels, as discussed in Section 3, the combined prediction reflects

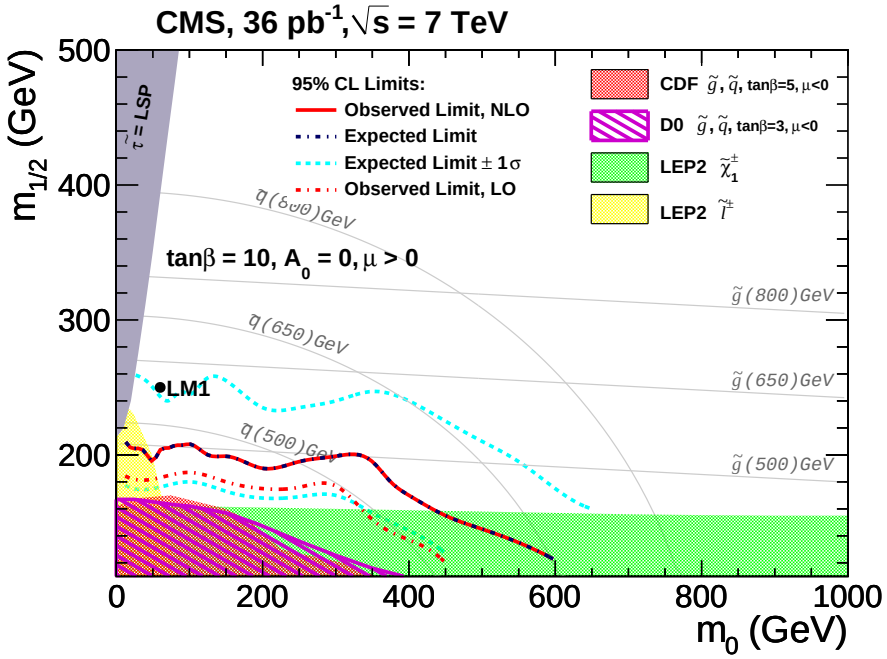

Figure 6: Exclusion region in the CMSSM $m_{1/2}$ vs. m_0 plane for $\tan\beta = 10$, based on the loose selection of the lepton-spectrum method, using the combined electron and muon samples. The observed limit is given for both LO and NLO assumed cross sections of the SUSY model points. In addition to the observed limit, the expected limit under the assumption of no signal contribution and the $\pm 1\sigma$ limits are shown.

the fact that the uncertainties between these two channels are highly correlated.) Applying the Feldman-Cousins method [59], which takes into account the number of events in the control samples using the profile likelihood ratio [60] to handle nuisance parameters, yields a 95% confidence level (CL) upper limit of 20.4 signal events (loose selection) and 3.8 signal events (tight selection). The central value and ± 1 σ range of the expected limits are obtained by applying the same method to MC pseudo-experiments. For comparison, the SUSY LM0 model predicts 64 ± 1 events for the loose selection and 11.2 ± 0.3 events for the tight selection (e and μ channels combined). The LM1 model, for which the yields are 8.7 ± 0.1 events (loose, e+μ) and 4.2 ± 0.1 events (tight, e+μ), is at the edge of the sensitivity of the analysis.

To obtain a more comprehensive result, we perform scans of CMSSM models to determine whether a given set of parameters is excluded. The Monte Carlo samples are initially generated using leading-order cross sections; the predicted yields are corrected using process-dependent NLO cross sections evaluated with PROSPINO [61]. Figure 6 shows the limit curves resulting from the loose selection, evaluated in the $m_{1/2}$ vs. m_0 plane, with the values of the remaining CMSSM parameters fixed at $\tan\beta = 10$, $A_0 = 0$, and $\mu > 0$. The corresponding curves for the tight selection, which exclude a larger region, are shown in Fig. 7. For reference, the plots include curves of constant gluino and squark masses. The lines of constant gluino mass are approximately horizontal with $m(\tilde{g}) \approx 2.5\, m_{1/2}$. The lines of constant squark mass are strongly curved in the $m_{1/2}$ vs. m_0 plane. The total signal cross section decreases as a function of $m_{1/2}$ and m_0, roughly following the squark-mass contours.

The signal efficiency is defined for each model as the number of events passing the reconstructed-event selection, divided by the total number of SUSY events generated in the simulation, summing over all decay chains. (This definition of efficiency therefore incorporates the many dif-

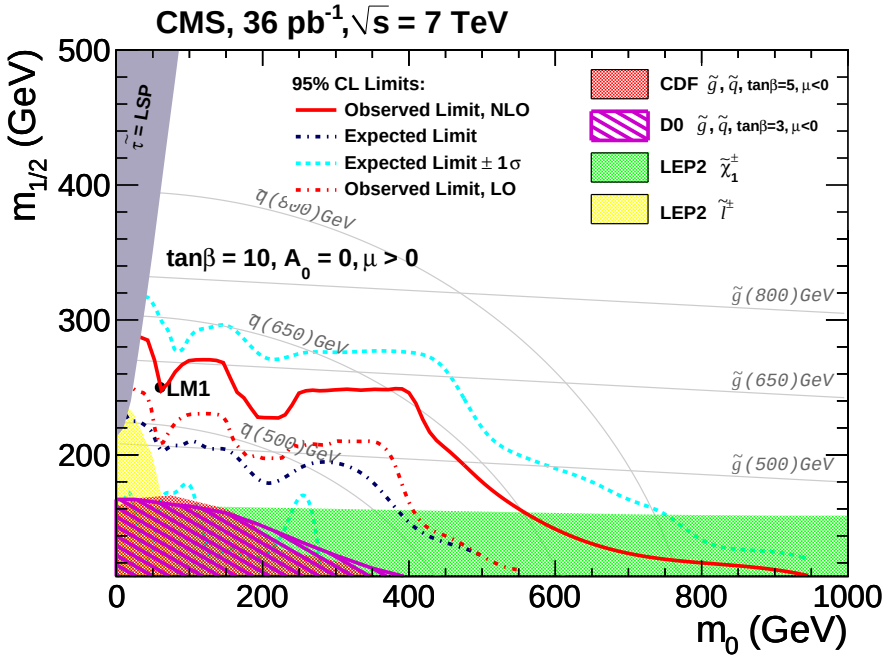

Figure 7: Exclusion region in the CMSSM $m_{1/2}$ vs. m_0 plane for $\tan\beta = 10$, based on the tight selection of the lepton-spectrum method, using the combined electron and muon samples.

ferent branching fractions leading to single-lepton final states, and it also includes the loss in efficiency associated with the dilepton veto.) The efficiency increases with $m_{1/2}$ but is relatively uniform as a function of m_0. In the tight selection, the efficiency in the combined e and μ channels is roughly 2% at $m_0 = 250$ GeV. For the benchmark model LM0 (LM1), the efficiency is 3.2% (3.6%) in the loose selection and 0.6% (1.7%) in the tight selection. If one were simply to require a reconstructed e or μ satisfying the acceptance requirements, the efficiency for LM1 would be 13%.

The exclusion plots show the observed limits, as well as the expected limits and the expected limits plus-or-minus one standard deviation ($\pm 1\sigma$). The loose selection has a smaller $\pm 1\sigma$ band and in fact provides a stronger exclusion of the low-mass part of the range. The small dips in the exclusion limits in the m_0 range 50–200 GeV arise from corresponding dips in the efficiency curves; the falloff in the exclusion limits around $m_0 = 350$–400 GeV is due to the decrease in the cross section. The tight selection excludes gluino masses below ≈600 GeV for m_0 below ≈400 GeV in the context of the CMSSM framework.

6 Conclusions

Using a sample of proton-proton collisions at $\sqrt{s} = 7$ TeV corresponding to an integrated luminosity of 36 pb^{-1}, we have performed a search for new physics with the experimental signature of at least four jets, an isolated, high-p_T lepton, and large missing transverse momentum. The overall shapes of the kinematic distributions observed in data are consistent with expectations from SM simulated event samples, indicating that the sample is dominated by $t\bar{t}$ and W+jets events.

To probe for new physics, control samples in the data are used to predict the background contributions in the signal region. The primary motivation for this approach is to avoid the direct

use of simulated background event samples for predicting the extreme tails of kinematic distributions. The first background determination method focuses on the jets and $\not\!\!E_{\mathrm{T}}$. Using the two-dimensional space of H_{T} and $\not\!\!E_{\mathrm{T}}/\sqrt{H_{\mathrm{T}}}$, three control regions are defined in data, from which one predicts the SM background in the fourth region. This region has both high H_{T} and high $\not\!\!E_{\mathrm{T}}/\sqrt{H_{\mathrm{T}}}$ and hence is most sensitive to a signal contribution. The observed event yield in the signal region is consistent with this prediction based on the control samples in the data.

The second method relies on the close relationship between two fundamental observables: the lepton p_{T} distribution and the $\not\!\!E_{\mathrm{T}}$ distribution, in the dominant SM background backgrounds with a single isolated lepton. This connection arises from the fact that the lepton and neutrino are produced together in the two-body decay of the W boson, for both $\mathrm{t\bar{t}}$ and W+jets events. Smaller backgrounds from the feed-down of $\mathrm{t\bar{t}}$ dilepton events, from $\tau \to \ell$ decays in $\mathrm{t\bar{t}}$ or W+jets events, and from QCD multijet processes are also estimated from control samples in the data. In the muon channel, we observe two events in the high-$\not\!\!E_{\mathrm{T}}$, high-H_{T} signal region (tight selection), as compared with $1.8 \pm 1.1 \pm 0.8$ SM events predicted; in the electron channel no events are observed, as compared with $1.4 \pm 0.9 \pm 0.5$ SM events predicted. The systematic uncertainties on the background predictions are correlated, and the total background prediction is 3.2 ± 2.3 events.

Finally, we interpret these results in the framework of the CMSSM, reporting exclusion regions as a function of $m_{1/2}$ and m_0, for $\tan\beta = 10$. The tight selection excludes gluino masses below $\approx$600 GeV for m_0 below $\approx$400 GeV in the context of the CMSSM framework.

Acknowledgments

We wish to congratulate our colleagues in the CERN accelerator departments for the excellent performance of the LHC machine. We thank the technical and administrative staff at CERN and other CMS institutes, and acknowledge support from: FMSR (Austria); FNRS and FWO (Belgium); CNPq, CAPES, FAPERJ, and FAPESP (Brazil); MES (Bulgaria); CERN; CAS, MoST, and NSFC (China); COLCIENCIAS (Colombia); MSES (Croatia); RPF (Cyprus); Academy of Sciences and NICPB (Estonia); Academy of Finland, MEC, and HIP (Finland); CEA and CNRS/IN2P3 (France); BMBF, DFG, and HGF (Germany); GSRT (Greece); OTKA and NKTH (Hungary); DAE and DST (India); IPM (Iran); SFI (Ireland); INFN (Italy); NRF and WCU (Korea); LAS (Lithuania); CINVESTAV, CONACYT, SEP, and UASLP-FAI (Mexico); MSI (New Zealand); PAEC (Pakistan); SCSR (Poland); FCT (Portugal); JINR (Armenia, Belarus, Georgia, Ukraine, Uzbekistan); MST, MAE and RFBR (Russia); MSTD (Serbia); MICINN and CPAN (Spain); Swiss Funding Agencies (Switzerland); NSC (Taipei); TUBITAK and TAEK (Turkey); STFC (United Kingdom); DOE and NSF (USA). Individuals have received support from the Marie-Curie programme and the European Research Council (European Union); the Leventis Foundation; the A. P. Sloan Foundation; the Alexander von Humboldt Foundation; the Associazione per lo Sviluppo Scientifico e Tecnologico del Piemonte (Italy); the Belgian Federal Science Policy Office; the Fonds pour la Formation à la Recherche dans l'Industrie et dans l'Agriculture (FRIA-Belgium); the Agentschap voor Innovatie door Wetenschap en Technologie (IWT-Belgium); and the Council of Science and Industrial Research, India.

References

[1] F. Zwicky, "Die Rotverschiebung von extragalaktischen Nebeln", *Helv. Physica Acta* **6** (1933) 110.

[2] V. Trimble, "The Existence and Nature of Dark Matter in the Universe", *Ann. Rev. Astron. Astrophys.* **25** (1987) 425. doi:10.1146/annurev.aa.25.090187.002233.

[3] M. Bartelmann, "The Dark Universe", *Rev. Mod. Phys.* **82** (2010) 1. doi:10.1103/RevModPhys.82.331.

[4] J. Feng, "Dark Matter Candidates from Particle Physics and Methods of Detection", *Ann. Rev. Astron. Astrophys.* **48** (2010) 495. doi:10.1146/annurev-astro-082708-101659.

[5] E. Witten, "Dynamical Breaking of Supersymmetry", *Nucl. Phys. B* **188** (1981) 513. doi:10.1016/0550-3213(81)90006-7.

[6] S. Dimopoulos and H. Georgi, "Softly Broken Supersymmetry and SU(5)", *Nucl. Phys. B* **193** (1981) 150. doi:10.1016/0550-3213(81)90522-8.

[7] CMS Collaboration, "Absolute Luminosity Normalization", CMS Detector Performance Summary CMS-DP-2011-003, (2011).

[8] J. Martin, "A Supersymmetry Primer", (1997). arXiv:9709356.

[9] J. Wess and B. Zumino, "Supergauge transformations in four dimensions", *Nucl. Phys. B* **70** (1974) 39. doi:10.1016/0550-3213(74)90355-1.

[10] H. P. Nilles, "Supersymmetry, Supergravity and Particle Physics", *Phys. Reports* **110** (1984) 1. doi:10.1016/0370-1573(84)90008-5.

[11] H. E. Haber and G. L. Kane, "The Search for Supersymmetry: Probing Physics Beyond the Standard Model", *Phys. Reports* **117** (1987) 75. doi:doi:10.1016/0370-1573(85)90051-1.

[12] R. Barbieri, S. Ferrara, and C. A. Savoy, "Gauge Models with Spontaneously Broken Local Supersymmetry", *Phys. Lett. B* **119** (1982) 343. doi:10.1016/0370-2693(82)90685-2.

[13] S. Dawson, E. Eichten, and C. Quigg, "Search for Supersymmetric Particles in Hadron - Hadron Collisions", *Phys. Rev. D* **31** (1985) 1581. doi:10.1103/PhysRevD.31.1581.

[14] CDF Collaboration, "Inclusive Search for Squark and Gluino Production in $p\bar{p}$ Collisions at $\sqrt{s} = 1.96\,\text{TeV}$", *Phys. Rev. Lett.* **102** (2009) 121801. doi:10.1103/PhysRevLett.102.121801.

[15] D0 Collaboration, "Search for squarks and gluinos in events with jets and missing transverse energy using 2.1 fb^{-1} of $p\bar{p}$ collision data at $\sqrt{s} = 1.96$ TeV", *Phys. Lett. B* **660** (2008) 449. doi:10.1016/j.physletb.2008.01.042.

[16] D0 Collaboration, "Search for associated production of charginos and neutralinos in the trilepton final state using 2.3 fb^{-1} of data", *Phys. Lett. B* **680** (2009) 34. doi:10.1016/j.physletb.2009.08.011.

[17] Joint SUSY Working Group (ALEPH, DELPHI, L3 and OPAL) Collaboration, "Interpretation of the results in Minimal SUGRA", (2002). LEPSUSYWG/02-06.2.

[18] ALEPH Collaboration, "Absolute mass lower limit for the lightest neutralino of the MSSM from e^+e^- data at $\sqrt{s}$ up to 209 GeV", *Phys. Lett. B* **583** (2004) 247. See also references therein. doi:10.1016/j.physletb.2003.12.066.

[19] DELPHI Collaboration, "Searches for supersymmetric particles in e^+e^- collisions up to 208 GeV and interpretation of the results within the MSSM", *Eur. Phys. J. C* **31** (2003) 421. See also references therein. doi:10.1140/epjc/s2003-01355-5.

[20] L3 Collaboration, "Search for scalar leptons and scalar quarks at LEP", *Phys. Lett. B* **580** (2004) 37. See also references therein. doi:10.1016/j.physletb.2003.10.010.

[21] OPAL Collaboration, "Search for chargino and neutralino production at $\sqrt{s} = 192 - 209$ GeV at LEP", *Eur. Phys. J. C* **35** (2004) 1. See also references therein. doi:10.1140/epjc/s2004-01758-8.

[22] CMS Collaboration, "Search for Supersymmetry in pp Collisions at 7 TeV in Events with Jets and Missing Transverse Energy", *Phys. Lett. B* **698** (2011) 196. doi:10.1016/j.physletb.2011.03.021.

[23] CMS Collaboration, "Search for Supersymmetry in pp Collisions at $\sqrt{s}$ = 7 TeV in Events with Two Photons and Missing Transverse Energy", (2011). arXiv:1103.0953. Submitted to Physical Review Letters.

[24] CMS Collaboration, "Search for new physics with same-sign isolated dilepton events with jets and missing transverse energy at the LHC", (2011). arXiv:1104.3168. Submitted to JHEP.

[25] CMS Collaboration, "Search for Physics Beyond the Standard Model in Opposite-sign Dilepton Events in pp Collisions at $\sqrt{s}$ = 7 TeV", (2011). arXiv:1103.1348. Submitted to JHEP.

[26] CMS Collaboration, "Search for supersymmetry in events with a lepton, a photon, and large missing transverse energy in pp collisions at $\sqrt{s}$ = 7 TeV", (2011). arXiv:1105.3152. Submitted to JHEP.

[27] CMS Collaboration, "Search for Physics Beyond the Standard Model Using Multilepton Signatures in pp Collisions at sqrt(s)=7 TeV", (2011). arXiv:1106.0933. Submitted to PLB.

[28] ATLAS Collaboration, "Search for supersymmetry using final states with one lepton, jets, and missing transverse momentum with the ATLAS detector in $\sqrt{s}$ = 7 TeV pp collisions", (2011). arXiv:1102.2357.

[29] ATLAS Collaboration, "Search for squarks and gluinos using final states with jets and missing transverse momentum with the ATLAS detector in $\sqrt{s}$ = 7 TeV proton-proton collisions", (2011). arXiv:1102.5290.

[30] ATLAS Collaboration, "Search for supersymmetry in pp collisions at $\sqrt{s}$ = 7 TeV in final states with missing transverse momentum and b-jets", (2011). arXiv:1103.4344.

[31] ATLAS Collaboration, "Search for supersymmetric particles in events with lepton pairs and large missing transverse momentum in $\sqrt{s}$ = 7 TeV proton-proton collisions at the ATLAS experiment", (2011). arXiv:1103.6214.

[32] ATLAS Collaboration, "Search for an excess of events with an identical flavour lepton pair and significant missing transverse momentum in $\sqrt{s}$ = 7 TeV proton-proton collisions with the ATLAS detector", (2011). arXiv:1103.6208.

[33] G. L. Kane, C. F. Kolda, L. Roszkowski et al., "Study of constrained minimal supersymmetry", *Phys. Rev. D* **49** (1994) 6173. doi:10.1103/PhysRevD.49.6173.

[34] A. H. Chamseddine, R. Arnowitt, and P. Nath, "Locally Supersymmetric Grand Unification", *Phys. Rev. Lett.* **49** (1982) 970. doi:10.1103/PhysRevLett.49.970.

[35] CMS Collaboration, "The CMS experiment at the CERN LHC", *JINST* **0803** (2008) S08004. doi:10.1088/1748-0221/3/08/S08004.

[36] GEANT4 Collaboration, "GEANT4: A simulation toolkit", *Nucl. Instrum. Meth. A* **506** (2003) 250. doi:10.1016/S0168-9002(03)01368-8.

[37] T. Sjöstrand, S. Mrenna, and P. Z. Skands, "PYTHIA 6.4 Physics and Manual; v6.420, tune D6T", *JHEP* **05** (2006) 026. doi:10.1088/1126-6708/2006/05/026.

[38] R. Field, "Early LHC underlying event data - findings and surprises", (2010). arXiv:1010.3558.

[39] J. Alwall et al., "MadGraph/MadEvent v4: The New Web Generation", *JHEP* **09** (2007) 028. doi:10.1088/1126-6708/2007/09/028.

[40] M.L. Mangano, M. Moretti, F. Piccinini, R. Pittau and A. Polosa, "ALPGEN, a generator for hard multiparton processes in hadronic collisions", *JHEP* **07** (2003) 001. doi:10.1088/1126-6708/2003/07/001.

[41] CMS Collaboration, "CMS technical design report, volume II: Physics performance", *J. Phys. G* **34** (2007) 995. doi:10.1088/0954-3899/34/6/S01.

[42] CMS Collaboration, "Particle–Flow Event Reconstruction in CMS and Performance for Jets, Taus, and $E_{\mathrm{T}}^{\mathrm{miss}}$", CMS Physics Analysis Summary CMS-PAS-PFT-09-001, (2009).

[43] CMS Collaboration, "Commissioning of the Particle-Flow Reconstruction in Minimum-Bias and Jet Events from pp Collisions at 7 TeV", CMS Physics Analysis Summary CMS-PAS-PFT-10-002, (2010).

[44] M. Cacciari, G. P. Salam, and G. Soyez, "The anti-k_{T} jet clustering algorithm", *JHEP* **0804** (2008) 063. doi:10.1088/1126-6708/2008/04/063.

[45] CMS Collaboration, "Jet Performance in pp Collisions at $\sqrt{s} = 7$ TeV", CMS Physics Analysis Summary JME-10-003, (2010).

[46] CMS Collaboration, "Determination of the Jet Energy Scale in CMS with pp Collisions at $\sqrt{s} = 7$ TeV", CMS Physics Analysis Summary CMS-PAS-JME-10-010, (2010).

[47] CMS Collaboration, "Performance of muon identification in pp collisions at $\sqrt{s}$ = 7 TeV", CMS Physics Analysis Summary CMS-PAS-MUO-10-002, (2010).

[48] CMS Collaboration, "Electron Reconstruction and Identification at $\sqrt{s} = 7$ TeV", CMS Physics Analysis Summary CMS-PAS-EGM-10-004, (2010).

[49] J. M. Campbell and R. K. Ellis, "Radiative corrections to Z b anti-b production", *Phys. Rev. D* **62** (2000) 114012. doi:10.1103/PhysRevD.62.114012.

[50] R. Kleiss and W. J. Stirling, "Top quark production at hadron colliders: Some useful formulae", *Z. Phys. C* **40** (1988) 419. doi:10.1007/BF01548856.

[51] K. Melnikov and F. Petriello, "Electroweak gauge boson production at hadron colliders through $O(\alpha_S^2)$", *Phys. Rev. D* **74** (2006) 114017. doi:10.1103/PhysRevD.74.114017.

[52] CMS Collaboration, "Measurement of the Top-antitop Production Cross Section at $\sqrt{s} = 7$ TeV using the Properties of Events with Leptons and Jets", (2011). arXiv:1106.0902. Submitted to EPJC.

[53] CMS Collaboration, "Missing transverse energy performance of the CMS detector", (2011). arXiv:1106.5048. Submitted to JINST.

[54] V. Pavlunin, "Modeling missing transverse energy in V+jets at the CERN LHC", (2009). arXiv:0906.5016.

[55] A. Czarnecki, J. Korner, and J. Piclum, "Helicity fractions of W bosons from top quark decays at next-to-next-to leading order in QCD", *Phys. Rev. D* **81** (2010) 111503(R). doi:10.1103/PhysRevD.81.111503.

[56] CDF Collaboration, "Measurement of W-Boson Polarization in Top-quark Decay in $p\bar{p}$ Collisions at $\sqrt{s} = 1.96$ TeV", *Phys. Rev. Lett.* **105** (2010) 042002. doi:10.1103/PhysRevLett.105.042002.

[57] CMS Collaboration, "Measurement of the Polarization of W Bosons with Large Transverse Momentum in W+Jets Events at the LHC", (2011). arXiv:1104.3829. Submitted to PRL.

[58] Z. Bern et al., "Left-handed W bosons at the LHC", (2011). arXiv:1103.5445.

[59] G. Feldman and R. Cousins, "Unified approach to the classical statistical analysis of small signals", *Phys. Rev. D* **57** (1998) 3873. doi:10.1103/PhysRevD.57.3873.

[60] T. A. Severini, "Likelihood methods in statistics", *Oxford University Press* (2000).

[61] W. Beenakker, R. Hopker, M. Spira et al., "Squark and gluino production at hadron colliders", *Nucl. Phys. B* **492** (1997) 51. doi:10.1016/S0550-3213(97)00084-9.

A The CMS Collaboration

Yerevan Physics Institute, Yerevan, Armenia
S. Chatrchyan, V. Khachatryan, A.M. Sirunyan, A. Tumasyan

Institut für Hochenergiephysik der OeAW, Wien, Austria
W. Adam, T. Bergauer, M. Dragicevic, J. Erö, C. Fabjan, M. Friedl, R. Frühwirth, V.M. Ghete, J. Hammer[1], S. Hänsel, M. Hoch, N. Hörmann, J. Hrubec, M. Jeitler, W. Kiesenhofer, M. Krammer, D. Liko, I. Mikulec, M. Pernicka, B. Rahbaran, H. Rohringer, R. Schöfbeck, J. Strauss, A. Taurok, F. Teischinger, P. Wagner, W. Waltenberger, G. Walzel, E. Widl, C.-E. Wulz

National Centre for Particle and High Energy Physics, Minsk, Belarus
V. Mossolov, N. Shumeiko, J. Suarez Gonzalez

Universiteit Antwerpen, Antwerpen, Belgium
S. Bansal, L. Benucci, E.A. De Wolf, X. Janssen, J. Maes, T. Maes, L. Mucibello, S. Ochesanu, B. Roland, R. Rougny, M. Selvaggi, H. Van Haevermaet, P. Van Mechelen, N. Van Remortel

Vrije Universiteit Brussel, Brussel, Belgium
F. Blekman, S. Blyweert, J. D'Hondt, O. Devroede, R. Gonzalez Suarez, A. Kalogeropoulos, M. Maes, W. Van Doninck, P. Van Mulders, G.P. Van Onsem, I. Villella

Université Libre de Bruxelles, Bruxelles, Belgium
O. Charaf, B. Clerbaux, G. De Lentdecker, V. Dero, A.P.R. Gay, G.H. Hammad, T. Hreus, P.E. Marage, L. Thomas, C. Vander Velde, P. Vanlaer

Ghent University, Ghent, Belgium
V. Adler, A. Cimmino, S. Costantini, M. Grunewald, B. Klein, J. Lellouch, A. Marinov, J. Mccartin, D. Ryckbosch, F. Thyssen, M. Tytgat, L. Vanelderen, P. Verwilligen, S. Walsh, N. Zaganidis

Université Catholique de Louvain, Louvain-la-Neuve, Belgium
S. Basegmez, G. Bruno, J. Caudron, L. Ceard, E. Cortina Gil, J. De Favereau De Jeneret, C. Delaere[1], D. Favart, A. Giammanco, G. Grégoire, J. Hollar, V. Lemaitre, J. Liao, O. Militaru, C. Nuttens, S. Ovyn, D. Pagano, A. Pin, K. Piotrzkowski, N. Schul

Université de Mons, Mons, Belgium
N. Beliy, T. Caebergs, E. Daubie

Centro Brasileiro de Pesquisas Fisicas, Rio de Janeiro, Brazil
G.A. Alves, L. Brito, D. De Jesus Damiao, M.E. Pol, M.H.G. Souza

Universidade do Estado do Rio de Janeiro, Rio de Janeiro, Brazil
W.L. Aldá Júnior, W. Carvalho, E.M. Da Costa, C. De Oliveira Martins, S. Fonseca De Souza, L. Mundim, H. Nogima, V. Oguri, W.L. Prado Da Silva, A. Santoro, S.M. Silva Do Amaral, A. Sznajder

Instituto de Fisica Teorica, Universidade Estadual Paulista, Sao Paulo, Brazil
C.A. Bernardes[2], F.A. Dias, T.R. Fernandez Perez Tomei, E. M. Gregores[2], C. Lagana, F. Marinho, P.G. Mercadante[2], S.F. Novaes, Sandra S. Padula

Institute for Nuclear Research and Nuclear Energy, Sofia, Bulgaria
N. Darmenov[1], V. Genchev[1], P. Iaydjiev[1], S. Piperov, M. Rodozov, S. Stoykova, G. Sultanov, V. Tcholakov, R. Trayanov

University of Sofia, Sofia, Bulgaria
A. Dimitrov, R. Hadjiiska, A. Karadzhinova, V. Kozhuharov, L. Litov, M. Mateev, B. Pavlov, P. Petkov

Institute of High Energy Physics, Beijing, China
J.G. Bian, G.M. Chen, H.S. Chen, C.H. Jiang, D. Liang, S. Liang, X. Meng, J. Tao, J. Wang, J. Wang, X. Wang, Z. Wang, H. Xiao, M. Xu, J. Zang, Z. Zhang

State Key Lab. of Nucl. Phys. and Tech., Peking University, Beijing, China
Y. Ban, S. Guo, Y. Guo, W. Li, Y. Mao, S.J. Qian, H. Teng, B. Zhu, W. Zou

Universidad de Los Andes, Bogota, Colombia
A. Cabrera, B. Gomez Moreno, A.A. Ocampo Rios, A.F. Osorio Oliveros, J.C. Sanabria

Technical University of Split, Split, Croatia
N. Godinovic, D. Lelas, K. Lelas, R. Plestina[3], D. Polic, I. Puljak

University of Split, Split, Croatia
Z. Antunovic, M. Dzelalija

Institute Rudjer Boskovic, Zagreb, Croatia
V. Brigljevic, S. Duric, K. Kadija, S. Morovic

University of Cyprus, Nicosia, Cyprus
A. Attikis, M. Galanti, J. Mousa, C. Nicolaou, F. Ptochos, P.A. Razis

Charles University, Prague, Czech Republic
M. Finger, M. Finger Jr.

Academy of Scientific Research and Technology of the Arab Republic of Egypt, Egyptian Network of High Energy Physics, Cairo, Egypt
Y. Assran[4], A. Ellithi Kamel, S. Khalil[5], M.A. Mahmoud[6]

National Institute of Chemical Physics and Biophysics, Tallinn, Estonia
A. Hektor, M. Kadastik, M. Müntel, M. Raidal, L. Rebane, A. Tiko

Department of Physics, University of Helsinki, Helsinki, Finland
V. Azzolini, P. Eerola, G. Fedi

Helsinki Institute of Physics, Helsinki, Finland
S. Czellar, J. Härkönen, A. Heikkinen, V. Karimäki, R. Kinnunen, M.J. Kortelainen, T. Lampén, K. Lassila-Perini, S. Lehti, T. Lindén, P. Luukka, T. Mäenpää, E. Tuominen, J. Tuominiemi, E. Tuovinen, D. Ungaro, L. Wendland

Lappeenranta University of Technology, Lappeenranta, Finland
K. Banzuzi, A. Karjalainen, A. Korpela, T. Tuuva

Laboratoire d'Annecy-le-Vieux de Physique des Particules, IN2P3-CNRS, Annecy-le-Vieux, France
D. Sillou

DSM/IRFU, CEA/Saclay, Gif-sur-Yvette, France
M. Besancon, S. Choudhury, M. Dejardin, D. Denegri, B. Fabbro, J.L. Faure, F. Ferri, S. Ganjour, F.X. Gentit, A. Givernaud, P. Gras, G. Hamel de Monchenault, P. Jarry, E. Locci, J. Malcles, M. Marionneau, L. Millischer, J. Rander, A. Rosowsky, I. Shreyber, M. Titov, P. Verrecchia

Laboratoire Leprince-Ringuet, Ecole Polytechnique, IN2P3-CNRS, Palaiseau, France
S. Baffioni, F. Beaudette, L. Benhabib, L. Bianchini, M. Bluj[7], C. Broutin, P. Busson, C. Charlot, T. Dahms, L. Dobrzynski, S. Elgammal, R. Granier de Cassagnac, M. Haguenauer, P. Miné, C. Mironov, C. Ochando, P. Paganini, D. Sabes, R. Salerno, Y. Sirois, C. Thiebaux, B. Wyslouch[8], A. Zabi

Institut Pluridisciplinaire Hubert Curien, Université de Strasbourg, Université de Haute Alsace Mulhouse, CNRS/IN2P3, Strasbourg, France
J.-L. Agram[9], J. Andrea, D. Bloch, D. Bodin, J.-M. Brom, M. Cardaci, E.C. Chabert, C. Collard, E. Conte[9], F. Drouhin[9], C. Ferro, J.-C. Fontaine[9], D. Gelé, U. Goerlach, S. Greder, P. Juillot, M. Karim[9], A.-C. Le Bihan, Y. Mikami, P. Van Hove

Centre de Calcul de l'Institut National de Physique Nucleaire et de Physique des Particules (IN2P3), Villeurbanne, France
F. Fassi, D. Mercier

Université de Lyon, Université Claude Bernard Lyon 1, CNRS-IN2P3, Institut de Physique Nucléaire de Lyon, Villeurbanne, France
C. Baty, S. Beauceron, N. Beaupere, M. Bedjidian, O. Bondu, G. Boudoul, D. Boumediene, H. Brun, J. Chasserat, R. Chierici, D. Contardo, P. Depasse, H. El Mamouni, J. Fay, S. Gascon, B. Ille, T. Kurca, T. Le Grand, M. Lethuillier, L. Mirabito, S. Perries, V. Sordini, S. Tosi, Y. Tschudi, P. Verdier

Institute of High Energy Physics and Informatization, Tbilisi State University, Tbilisi, Georgia
D. Lomidze

RWTH Aachen University, I. Physikalisches Institut, Aachen, Germany
G. Anagnostou, S. Beranek, M. Edelhoff, L. Feld, N. Heracleous, O. Hindrichs, R. Jussen, K. Klein, J. Merz, N. Mohr, A. Ostapchuk, A. Perieanu, F. Raupach, J. Sammet, S. Schael, D. Sprenger, H. Weber, M. Weber, B. Wittmer

RWTH Aachen University, III. Physikalisches Institut A, Aachen, Germany
M. Ata, E. Dietz-Laursonn, M. Erdmann, T. Hebbeker, C. Heidemann, A. Hinzmann, K. Hoepfner, T. Klimkovich, D. Klingebiel, P. Kreuzer, D. Lanske†, J. Lingemann, C. Magass, M. Merschmeyer, A. Meyer, P. Papacz, H. Pieta, H. Reithler, S.A. Schmitz, L. Sonnenschein, J. Steggemann, D. Teyssier

RWTH Aachen University, III. Physikalisches Institut B, Aachen, Germany
M. Bontenackels, M. Davids, M. Duda, G. Flügge, H. Geenen, M. Giffels, W. Haj Ahmad, D. Heydhausen, F. Hoehle, B. Kargoll, T. Kress, Y. Kuessel, A. Linn, A. Nowack, L. Perchalla, O. Pooth, J. Rennefeld, P. Sauerland, A. Stahl, M. Thomas, D. Tornier, M.H. Zoeller

Deutsches Elektronen-Synchrotron, Hamburg, Germany
M. Aldaya Martin, W. Behrenhoff, U. Behrens, M. Bergholz[10], A. Bethani, K. Borras, A. Cakir, A. Campbell, E. Castro, D. Dammann, G. Eckerlin, D. Eckstein, A. Flossdorf, G. Flucke, A. Geiser, J. Hauk, H. Jung[1], M. Kasemann, I. Katkov[11], P. Katsas, C. Kleinwort, H. Kluge, A. Knutsson, M. Krämer, D. Krücker, E. Kuznetsova, W. Lange, W. Lohmann[10], R. Mankel, M. Marienfeld, I.-A. Melzer-Pellmann, A.B. Meyer, J. Mnich, A. Mussgiller, J. Olzem, A. Petrukhin, D. Pitzl, A. Raspereza, A. Raval, M. Rosin, R. Schmidt[10], T. Schoerner-Sadenius, N. Sen, A. Spiridonov, M. Stein, J. Tomaszewska, R. Walsh, C. Wissing

University of Hamburg, Hamburg, Germany
C. Autermann, V. Blobel, S. Bobrovskyi, J. Draeger, H. Enderle, U. Gebbert, M. Görner,

T. Hermanns, K. Kaschube, G. Kaussen, H. Kirschenmann, R. Klanner, J. Lange, B. Mura, S. Naumann-Emme, F. Nowak, N. Pietsch, C. Sander, H. Schettler, P. Schleper, E. Schlieckau, M. Schröder, T. Schum, H. Stadie, G. Steinbrück, J. Thomsen

Institut für Experimentelle Kernphysik, Karlsruhe, Germany
C. Barth, J. Bauer, J. Berger, V. Buege, T. Chwalek, W. De Boer, A. Dierlamm, G. Dirkes, M. Feindt, J. Gruschke, C. Hackstein, F. Hartmann, M. Heinrich, H. Held, K.H. Hoffmann, S. Honc, J.R. Komaragiri, T. Kuhr, D. Martschei, S. Mueller, Th. Müller, M. Niegel, O. Oberst, A. Oehler, J. Ott, T. Peiffer, G. Quast, K. Rabbertz, F. Ratnikov, N. Ratnikova, M. Renz, C. Saout, A. Scheurer, P. Schieferdecker, F.-P. Schilling, G. Schott, H.J. Simonis, F.M. Stober, D. Troendle, J. Wagner-Kuhr, T. Weiler, M. Zeise, V. Zhukov[11], E.B. Ziebarth

Institute of Nuclear Physics "Demokritos", Aghia Paraskevi, Greece
G. Daskalakis, T. Geralis, S. Kesisoglou, A. Kyriakis, D. Loukas, I. Manolakos, A. Markou, C. Markou, C. Mavrommatis, E. Ntomari, E. Petrakou

University of Athens, Athens, Greece
L. Gouskos, T.J. Mertzimekis, A. Panagiotou, E. Stiliaris

University of Ioánnina, Ioánnina, Greece
I. Evangelou, C. Foudas, P. Kokkas, N. Manthos, I. Papadopoulos, V. Patras, F.A. Triantis

KFKI Research Institute for Particle and Nuclear Physics, Budapest, Hungary
A. Aranyi, G. Bencze, L. Boldizsar, C. Hajdu[1], P. Hidas, D. Horvath[12], A. Kapusi, K. Krajczar[13], F. Sikler[1], G.I. Veres[13], G. Vesztergombi[13]

Institute of Nuclear Research ATOMKI, Debrecen, Hungary
N. Beni, J. Molnar, J. Palinkas, Z. Szillasi, V. Veszpremi

University of Debrecen, Debrecen, Hungary
P. Raics, Z.L. Trocsanyi, B. Ujvari

Panjab University, Chandigarh, India
S.B. Beri, V. Bhatnagar, N. Dhingra, R. Gupta, M. Jindal, M. Kaur, J.M. Kohli, M.Z. Mehta, N. Nishu, L.K. Saini, A. Sharma, A.P. Singh, J. Singh, S.P. Singh

University of Delhi, Delhi, India
S. Ahuja, B.C. Choudhary, P. Gupta, S. Jain, A. Kumar, A. Kumar, M. Naimuddin, K. Ranjan, R.K. Shivpuri

Saha Institute of Nuclear Physics, Kolkata, India
S. Banerjee, S. Bhattacharya, S. Dutta, B. Gomber, S. Jain, R. Khurana, S. Sarkar

Bhabha Atomic Research Centre, Mumbai, India
R.K. Choudhury, D. Dutta, S. Kailas, V. Kumar, P. Mehta, A.K. Mohanty[1], L.M. Pant, P. Shukla

Tata Institute of Fundamental Research - EHEP, Mumbai, India
T. Aziz, M. Guchait[14], A. Gurtu, M. Maity[15], D. Majumder, G. Majumder, K. Mazumdar, G.B. Mohanty, A. Saha, K. Sudhakar, N. Wickramage

Tata Institute of Fundamental Research - HECR, Mumbai, India
S. Banerjee, S. Dugad, N.K. Mondal

Institute for Research and Fundamental Sciences (IPM), Tehran, Iran
H. Arfaei, H. Bakhshiansohi[16], S.M. Etesami, A. Fahim[16], M. Hashemi, H. Hesari, A. Jafari[16],

M. Khakzad, A. Mohammadi[17], M. Mohammadi Najafabadi, S. Paktinat Mehdiabadi, B. Safarzadeh, M. Zeinali[18]

INFN Sezione di Bari [a], Università di Bari [b], Politecnico di Bari [c], Bari, Italy
M. Abbrescia[a,b], L. Barbone[a,b], C. Calabria[a,b], A. Colaleo[a], D. Creanza[a,c], N. De Filippis[a,c,1], M. De Palma[a,b], L. Fiore[a], G. Iaselli[a,c], L. Lusito[a,b], G. Maggi[a,c], M. Maggi[a], N. Manna[a,b], B. Marangelli[a,b], S. My[a,c], S. Nuzzo[a,b], N. Pacifico[a,b], G.A. Pierro[a], A. Pompili[a,b], G. Pugliese[a,c], F. Romano[a,c], G. Roselli[a,b], G. Selvaggi[a,b], L. Silvestris[a], R. Trentadue[a], S. Tupputi[a,b], G. Zito[a]

INFN Sezione di Bologna [a], Università di Bologna [b], Bologna, Italy
G. Abbiendi[a], A.C. Benvenuti[a], D. Bonacorsi[a], S. Braibant-Giacomelli[a,b], L. Brigliadori[a], P. Capiluppi[a,b], A. Castro[a,b], F.R. Cavallo[a], M. Cuffiani[a,b], G.M. Dallavalle[a], F. Fabbri[a], A. Fanfani[a,b], D. Fasanella[a], P. Giacomelli[a], M. Giunta[a], C. Grandi[a], S. Marcellini[a], G. Masetti[b], M. Meneghelli[a,b], A. Montanari[a], F.L. Navarria[a,b], F. Odorici[a], A. Perrotta[a], F. Primavera[a], A.M. Rossi[a,b], T. Rovelli[a,b], G. Siroli[a,b], R. Travaglini[a,b]

INFN Sezione di Catania [a], Università di Catania [b], Catania, Italy
S. Albergo[a,b], G. Cappello[a,b], M. Chiorboli[a,b,1], S. Costa[a,b], A. Tricomi[a,b], C. Tuve[a,b]

INFN Sezione di Firenze [a], Università di Firenze [b], Firenze, Italy
G. Barbagli[a], V. Ciulli[a,b], C. Civinini[a], R. D'Alessandro[a,b], E. Focardi[a,b], S. Frosali[a,b], E. Gallo[a], S. Gonzi[a,b], P. Lenzi[a,b], M. Meschini[a], S. Paoletti[a], G. Sguazzoni[a], A. Tropiano[a,1]

INFN Laboratori Nazionali di Frascati, Frascati, Italy
L. Benussi, S. Bianco, S. Colafranceschi[19], F. Fabbri, D. Piccolo

INFN Sezione di Genova, Genova, Italy
P. Fabbricatore, R. Musenich

INFN Sezione di Milano-Bicocca [a], Università di Milano-Bicocca [b], Milano, Italy
A. Benaglia[a,b], F. De Guio[a,b,1], L. Di Matteo[a,b], S. Gennai[1], A. Ghezzi[a,b], S. Malvezzi[a], A. Martelli[a,b], A. Massironi[a,b], D. Menasce[a], L. Moroni[a], M. Paganoni[a,b], D. Pedrini[a], S. Ragazzi[a,b], N. Redaelli[a], S. Sala[a], T. Tabarelli de Fatis[a,b]

INFN Sezione di Napoli [a], Università di Napoli "Federico II" [b], Napoli, Italy
S. Buontempo[a], C.A. Carrillo Montoya[a,1], N. Cavallo[a,20], A. De Cosa[a,b], F. Fabozzi[a,20], A.O.M. Iorio[a,1], L. Lista[a], M. Merola[a,b], P. Paolucci[a]

INFN Sezione di Padova [a], Università di Padova [b], Università di Trento (Trento) [c], Padova, Italy
P. Azzi[a], N. Bacchetta[a], P. Bellan[a,b], D. Bisello[a,b], A. Branca[a], R. Carlin[a,b], P. Checchia[a], T. Dorigo[a], U. Dosselli[a], F. Gasparini[a,b], U. Gasparini[a,b], A. Gozzelino, S. Lacaprara[a,21], I. Lazzizzera[a,c], M. Margoni[a,b], M. Mazzucato[a], A.T. Meneguzzo[a,b], M. Nespolo[a,1], M. Passaseo[a], L. Perrozzi[a,1], N. Pozzobon[a,b], P. Ronchese[a,b], F. Simonetto[a,b], E. Torassa[a], M. Tosi[a,b], S. Vanini[a,b], P. Zotto[a,b], G. Zumerle[a,b]

INFN Sezione di Pavia [a], Università di Pavia [b], Pavia, Italy
P. Baesso[a,b], U. Berzano[a], S.P. Ratti[a,b], C. Riccardi[a,b], P. Torre[a,b], P. Vitulo[a,b], C. Viviani[a,b]

INFN Sezione di Perugia [a], Università di Perugia [b], Perugia, Italy
M. Biasini[a,b], G.M. Bilei[a], B. Caponeri[a,b], L. Fanò[a,b], P. Lariccia[a,b], A. Lucaroni[a,b,1], G. Mantovani[a,b], M. Menichelli[a], A. Nappi[a,b], F. Romeo[a,b], A. Santocchia[a,b], S. Taroni[a,b,1], M. Valdata[a,b]

INFN Sezione di Pisa [a], Università di Pisa [b], Scuola Normale Superiore di Pisa [c], Pisa, Italy
P. Azzurri[a,c], G. Bagliesi[a], J. Bernardini[a,b], T. Boccali[a,1], G. Broccolo[a,c], R. Castaldi[a], R.T. D'Agnolo[a,c], R. Dell'Orso[a], F. Fiori[a,b], L. Foà[a,c], A. Giassi[a], A. Kraan[a], F. Ligabue[a,c], T. Lomtadze[a], L. Martini[a,22], A. Messineo[a,b], F. Palla[a], G. Segneri[a], A.T. Serban[a], P. Spagnolo[a], R. Tenchini[a], G. Tonelli[a,b,1], A. Venturi[a,1], P.G. Verdini[a]

INFN Sezione di Roma [a], Università di Roma "La Sapienza" [b], Roma, Italy
L. Barone[a,b], F. Cavallari[a], D. Del Re[a,b], E. Di Marco[a,b], M. Diemoz[a], D. Franci[a,b], M. Grassi[a,1], E. Longo[a,b], P. Meridiani, S. Nourbakhsh[a], G. Organtini[a,b], F. Pandolfi[a,b,1], R. Paramatti[a], S. Rahatlou[a,b], C. Rovelli[1]

INFN Sezione di Torino [a], Università di Torino [b], Università del Piemonte Orientale (Novara) [c], Torino, Italy
N. Amapane[a,b], R. Arcidiacono[a,c], S. Argiro[a,b], M. Arneodo[a,c], C. Biino[a], C. Botta[a,b,1], N. Cartiglia[a], R. Castello[a,b], M. Costa[a,b], N. Demaria[a], A. Graziano[a,b,1], C. Mariotti[a], M. Marone[a,b], S. Maselli[a], E. Migliore[a,b], G. Mila[a,b], V. Monaco[a,b], M. Musich[a,b], M.M. Obertino[a,c], N. Pastrone[a], M. Pelliccioni[a,b], A. Potenza[a,b], A. Romero[a,b], M. Ruspa[a,c], R. Sacchi[a,b], V. Sola[a,b], A. Solano[a,b], A. Staiano[a], A. Vilela Pereira[a]

INFN Sezione di Trieste [a], Università di Trieste [b], Trieste, Italy
S. Belforte[a], F. Cossutti[a], G. Della Ricca[a,b], B. Gobbo[a], D. Montanino[a,b], A. Penzo[a]

Kangwon National University, Chunchon, Korea
S.G. Heo, S.K. Nam

Kyungpook National University, Daegu, Korea
S. Chang, J. Chung, D.H. Kim, G.N. Kim, J.E. Kim, D.J. Kong, H. Park, S.R. Ro, D. Son, D.C. Son, T. Son

Chonnam National University, Institute for Universe and Elementary Particles, Kwangju, Korea
Zero Kim, J.Y. Kim, S. Song

Korea University, Seoul, Korea
S. Choi, B. Hong, M. Jo, H. Kim, J.H. Kim, T.J. Kim, K.S. Lee, D.H. Moon, S.K. Park, K.S. Sim

University of Seoul, Seoul, Korea
M. Choi, S. Kang, H. Kim, C. Park, I.C. Park, S. Park, G. Ryu

Sungkyunkwan University, Suwon, Korea
Y. Choi, Y.K. Choi, J. Goh, M.S. Kim, J. Lee, S. Lee, H. Seo, I. Yu

Vilnius University, Vilnius, Lithuania
M.J. Bilinskas, I. Grigelionis, M. Janulis, D. Martisiute, P. Petrov, T. Sabonis

Centro de Investigacion y de Estudios Avanzados del IPN, Mexico City, Mexico
H. Castilla-Valdez, E. De La Cruz-Burelo, I. Heredia-de La Cruz, R. Lopez-Fernandez, R. Magaña Villalba, A. Sánchez-Hernández, L.M. Villasenor-Cendejas

Universidad Iberoamericana, Mexico City, Mexico
S. Carrillo Moreno, F. Vazquez Valencia

Benemerita Universidad Autonoma de Puebla, Puebla, Mexico
H.A. Salazar Ibarguen

Universidad Autónoma de San Luis Potosí, San Luis Potosí, Mexico
E. Casimiro Linares, A. Morelos Pineda, M.A. Reyes-Santos

University of Auckland, Auckland, New Zealand
D. Krofcheck, J. Tam

University of Canterbury, Christchurch, New Zealand
P.H. Butler, R. Doesburg, H. Silverwood

National Centre for Physics, Quaid-I-Azam University, Islamabad, Pakistan
M. Ahmad, I. Ahmed, M.I. Asghar, H.R. Hoorani, W.A. Khan, T. Khurshid, S. Qazi

Institute of Experimental Physics, Faculty of Physics, University of Warsaw, Warsaw, Poland
G. Brona, M. Cwiok, W. Dominik, K. Doroba, A. Kalinowski, M. Konecki, J. Krolikowski

Soltan Institute for Nuclear Studies, Warsaw, Poland
T. Frueboes, R. Gokieli, M. Górski, M. Kazana, K. Nawrocki, K. Romanowska-Rybinska, M. Szleper, G. Wrochna, P. Zalewski

Laboratório de Instrumentação e Física Experimental de Partículas, Lisboa, Portugal
N. Almeida, P. Bargassa, A. David, P. Faccioli, P.G. Ferreira Parracho, M. Gallinaro, P. Musella, A. Nayak, J. Pela[1], P.Q. Ribeiro, J. Seixas, J. Varela

Joint Institute for Nuclear Research, Dubna, Russia
S. Afanasiev, I. Belotelov, P. Bunin, I. Golutvin, V. Karjavin, G. Kozlov, A. Lanev, P. Moisenz, V. Palichik, V. Perelygin, M. Savina, S. Shmatov, V. Smirnov, A. Volodko, A. Zarubin

Petersburg Nuclear Physics Institute, Gatchina (St Petersburg), Russia
V. Golovtsov, Y. Ivanov, V. Kim, P. Levchenko, V. Murzin, V. Oreshkin, I. Smirnov, V. Sulimov, L. Uvarov, S. Vavilov, A. Vorobyev, An. Vorobyev

Institute for Nuclear Research, Moscow, Russia
Yu. Andreev, A. Dermenev, S. Gninenko, N. Golubev, M. Kirsanov, N. Krasnikov, V. Matveev, A. Pashenkov, A. Toropin, S. Troitsky

Institute for Theoretical and Experimental Physics, Moscow, Russia
V. Epshteyn, V. Gavrilov, V. Kaftanov†, M. Kossov[1], A. Krokhotin, N. Lychkovskaya, V. Popov, G. Safronov, S. Semenov, V. Stolin, E. Vlasov, A. Zhokin

Moscow State University, Moscow, Russia
E. Boos, M. Dubinin[23], L. Dudko, A. Ershov, A. Gribushin, O. Kodolova, I. Lokhtin, A. Markina, S. Obraztsov, M. Perfilov, S. Petrushanko, L. Sarycheva, V. Savrin, A. Snigirev

P.N. Lebedev Physical Institute, Moscow, Russia
V. Andreev, M. Azarkin, I. Dremin, M. Kirakosyan, A. Leonidov, S.V. Rusakov, A. Vinogradov

State Research Center of Russian Federation, Institute for High Energy Physics, Protvino, Russia
I. Azhgirey, I. Bayshev, S. Bitioukov, V. Grishin[1], V. Kachanov, D. Konstantinov, A. Korablev, V. Krychkine, V. Petrov, R. Ryutin, A. Sobol, L. Tourtchanovitch, S. Troshin, N. Tyurin, A. Uzunian, A. Volkov

University of Belgrade, Faculty of Physics and Vinca Institute of Nuclear Sciences, Belgrade, Serbia
P. Adzic[24], M. Djordjevic, D. Krpic[24], J. Milosevic

Centro de Investigaciones Energéticas Medioambientales y Tecnológicas (CIEMAT), Madrid, Spain
M. Aguilar-Benitez, J. Alcaraz Maestre, P. Arce, C. Battilana, E. Calvo, M. Cepeda, M. Cerrada, M. Chamizo Llatas, N. Colino, B. De La Cruz, A. Delgado Peris, C. Diez Pardos, D. Domínguez Vázquez, C. Fernandez Bedoya, J.P. Fernández Ramos, A. Ferrando, J. Flix, M.C. Fouz, P. Garcia-Abia, O. Gonzalez Lopez, S. Goy Lopez, J.M. Hernandez, M.I. Josa, G. Merino, J. Puerta Pelayo, I. Redondo, L. Romero, J. Santaolalla, M.S. Soares, C. Willmott

Universidad Autónoma de Madrid, Madrid, Spain
C. Albajar, G. Codispoti, J.F. de Trocóniz

Universidad de Oviedo, Oviedo, Spain
J. Cuevas, J. Fernandez Menendez, S. Folgueras, I. Gonzalez Caballero, L. Lloret Iglesias, J.M. Vizan Garcia

Instituto de Física de Cantabria (IFCA), CSIC-Universidad de Cantabria, Santander, Spain
J.A. Brochero Cifuentes, I.J. Cabrillo, A. Calderon, S.H. Chuang, J. Duarte Campderros, M. Felcini[25], M. Fernandez, G. Gomez, J. Gonzalez Sanchez, C. Jorda, P. Lobelle Pardo, A. Lopez Virto, J. Marco, R. Marco, C. Martinez Rivero, F. Matorras, F.J. Munoz Sanchez, J. Piedra Gomez[26], T. Rodrigo, A.Y. Rodríguez-Marrero, A. Ruiz-Jimeno, L. Scodellaro, M. Sobron Sanudo, I. Vila, R. Vilar Cortabitarte

CERN, European Organization for Nuclear Research, Geneva, Switzerland
D. Abbaneo, E. Auffray, G. Auzinger, P. Baillon, A.H. Ball, D. Barney, A.J. Bell[27], D. Benedetti, C. Bernet[3], W. Bialas, P. Bloch, A. Bocci, S. Bolognesi, M. Bona, H. Breuker, K. Bunkowski, T. Camporesi, G. Cerminara, T. Christiansen, J.A. Coarasa Perez, B. Curé, D. D'Enterria, A. De Roeck, S. Di Guida, N. Dupont-Sagorin, A. Elliott-Peisert, B. Frisch, W. Funk, A. Gaddi, G. Georgiou, H. Gerwig, D. Gigi, K. Gill, D. Giordano, F. Glege, R. Gomez-Reino Garrido, M. Gouzevitch, P. Govoni, S. Gowdy, L. Guiducci, M. Hansen, C. Hartl, J. Harvey, J. Hegeman, B. Hegner, H.F. Hoffmann, A. Honma, V. Innocente, P. Janot, K. Kaadze, E. Karavakis, P. Lecoq, C. Lourenço, T. Mäki, M. Malberti, L. Malgeri, M. Mannelli, L. Masetti, A. Maurisset, F. Meijers, S. Mersi, E. Meschi, R. Moser, M.U. Mozer, M. Mulders, E. Nesvold[1], M. Nguyen, T. Orimoto, L. Orsini, E. Palencia Cortezon, E. Perez, A. Petrilli, A. Pfeiffer, M. Pierini, M. Pimiä, D. Piparo, G. Polese, A. Racz, W. Reece, J. Rodrigues Antunes, G. Rolandi[28], T. Rommerskirchen, M. Rovere, H. Sakulin, C. Schäfer, C. Schwick, I. Segoni, A. Sharma, P. Siegrist, P. Silva, M. Simon, P. Sphicas[29], M. Spiropulu[23], M. Stoye, P. Tropea, A. Tsirou, P. Vichoudis, M. Voutilainen, W.D. Zeuner

Paul Scherrer Institut, Villigen, Switzerland
W. Bertl, K. Deiters, W. Erdmann, K. Gabathuler, R. Horisberger, Q. Ingram, H.C. Kaestli, S. König, D. Kotlinski, U. Langenegger, F. Meier, D. Renker, T. Rohe, J. Sibille[30], A. Starodumov[31]

Institute for Particle Physics, ETH Zurich, Zurich, Switzerland
L. Bäni, P. Bortignon, L. Caminada[32], B. Casal, N. Chanon, Z. Chen, S. Cittolin, G. Dissertori, M. Dittmar, J. Eugster, K. Freudenreich, C. Grab, W. Hintz, P. Lecomte, W. Lustermann, C. Marchica[32], P. Martinez Ruiz del Arbol, P. Milenovic[33], F. Moortgat, C. Nägeli[32], P. Nef, F. Nessi-Tedaldi, L. Pape, F. Pauss, T. Punz, A. Rizzi, F.J. Ronga, M. Rossini, L. Sala, A.K. Sanchez, M.-C. Sawley, B. Stieger, L. Tauscher†, A. Thea, K. Theofilatos, D. Treille, C. Urscheler, R. Wallny, M. Weber, L. Wehrli, J. Weng

Universität Zürich, Zurich, Switzerland

E. Aguilo, C. Amsler, V. Chiochia, S. De Visscher, C. Favaro, M. Ivova Rikova, B. Millan Mejias, P. Otiougova, C. Regenfus, P. Robmann, A. Schmidt, H. Snoek

National Central University, Chung-Li, Taiwan
Y.H. Chang, K.H. Chen, C.M. Kuo, S.W. Li, W. Lin, Z.K. Liu, Y.J. Lu, D. Mekterovic, R. Volpe, J.H. Wu, S.S. Yu

National Taiwan University (NTU), Taipei, Taiwan
P. Bartalini, P. Chang, Y.H. Chang, Y.W. Chang, Y. Chao, K.F. Chen, W.-S. Hou, Y. Hsiung, K.Y. Kao, Y.J. Lei, R.-S. Lu, J.G. Shiu, Y.M. Tzeng, M. Wang

Cukurova University, Adana, Turkey
A. Adiguzel, M.N. Bakirci[34], S. Cerci[35], C. Dozen, I. Dumanoglu, E. Eskut, S. Girgis, G. Gokbulut, I. Hos, E.E. Kangal, A. Kayis Topaksu, G. Onengut, K. Ozdemir, S. Ozturk[36], A. Polatoz, K. Sogut[37], D. Sunar Cerci[35], B. Tali[35], H. Topakli[34], D. Uzun, L.N. Vergili, M. Vergili

Middle East Technical University, Physics Department, Ankara, Turkey
I.V. Akin, T. Aliev, B. Bilin, S. Bilmis, M. Deniz, H. Gamsizkan, A.M. Guler, K. Ocalan, A. Ozpineci, M. Serin, R. Sever, U.E. Surat, E. Yildirim, M. Zeyrek

Bogazici University, Istanbul, Turkey
M. Deliomeroglu, D. Demir[38], E. Gülmez, B. Isildak, M. Kaya[39], O. Kaya[39], M. Özbek, S. Ozkorucuklu[40], N. Sonmez[41]

National Scientific Center, Kharkov Institute of Physics and Technology, Kharkov, Ukraine
L. Levchuk

University of Bristol, Bristol, United Kingdom
F. Bostock, J.J. Brooke, T.L. Cheng, E. Clement, D. Cussans, R. Frazier, J. Goldstein, M. Grimes, D. Hartley, G.P. Heath, H.F. Heath, L. Kreczko, S. Metson, D.M. Newbold[42], K. Nirunpong, A. Poll, S. Senkin, V.J. Smith

Rutherford Appleton Laboratory, Didcot, United Kingdom
L. Basso[43], K.W. Bell, A. Belyaev[43], C. Brew, R.M. Brown, B. Camanzi, D.J.A. Cockerill, J.A. Coughlan, K. Harder, S. Harper, J. Jackson, B.W. Kennedy, E. Olaiya, D. Petyt, B.C. Radburn-Smith, C.H. Shepherd-Themistocleous, I.R. Tomalin, W.J. Womersley, S.D. Worm

Imperial College, London, United Kingdom
R. Bainbridge, G. Ball, J. Ballin, R. Beuselinck, O. Buchmuller, D. Colling, N. Cripps, M. Cutajar, G. Davies, M. Della Negra, W. Ferguson, J. Fulcher, D. Futyan, A. Gilbert, A. Guneratne Bryer, G. Hall, Z. Hatherell, J. Hays, G. Iles, M. Jarvis, G. Karapostoli, L. Lyons, B.C. MacEvoy, A.-M. Magnan, J. Marrouche, B. Mathias, R. Nandi, J. Nash, A. Nikitenko[31], A. Papageorgiou, M. Pesaresi, K. Petridis, M. Pioppi[44], D.M. Raymond, S. Rogerson, N. Rompotis, A. Rose, M.J. Ryan, C. Seez, P. Sharp, A. Sparrow, A. Tapper, S. Tourneur, M. Vazquez Acosta, T. Virdee, S. Wakefield, N. Wardle, D. Wardrope, T. Whyntie

Brunel University, Uxbridge, United Kingdom
M. Barrett, M. Chadwick, J.E. Cole, P.R. Hobson, A. Khan, P. Kyberd, D. Leslie, W. Martin, I.D. Reid, L. Teodorescu

Baylor University, Waco, USA
K. Hatakeyama, H. Liu

The University of Alabama, Tuscaloosa, USA
C. Henderson

Boston University, Boston, USA
T. Bose, E. Carrera Jarrin, C. Fantasia, A. Heister, J. St. John, P. Lawson, D. Lazic, J. Rohlf, D. Sperka, L. Sulak

Brown University, Providence, USA
A. Avetisyan, S. Bhattacharya, J.P. Chou, D. Cutts, A. Ferapontov, U. Heintz, S. Jabeen, G. Kukartsev, G. Landsberg, M. Luk, M. Narain, D. Nguyen, M. Segala, T. Sinthuprasith, T. Speer, K.V. Tsang

University of California, Davis, Davis, USA
R. Breedon, G. Breto, M. Calderon De La Barca Sanchez, S. Chauhan, M. Chertok, J. Conway, P.T. Cox, J. Dolen, R. Erbacher, E. Friis, W. Ko, A. Kopecky, R. Lander, H. Liu, S. Maruyama, T. Miceli, M. Nikolic, D. Pellett, J. Robles, S. Salur, T. Schwarz, M. Searle, J. Smith, M. Squires, M. Tripathi, R. Vasquez Sierra, C. Veelken

University of California, Los Angeles, Los Angeles, USA
V. Andreev, K. Arisaka, D. Cline, R. Cousins, A. Deisher, J. Duris, S. Erhan, C. Farrell, J. Hauser, M. Ignatenko, C. Jarvis, C. Plager, G. Rakness, P. Schlein†, J. Tucker, V. Valuev

University of California, Riverside, Riverside, USA
J. Babb, A. Chandra, R. Clare, J. Ellison, J.W. Gary, F. Giordano, G. Hanson, G.Y. Jeng, S.C. Kao, F. Liu, H. Liu, O.R. Long, A. Luthra, H. Nguyen, B.C. Shen†, R. Stringer, J. Sturdy, S. Sumowidagdo, R. Wilken, S. Wimpenny

University of California, San Diego, La Jolla, USA
W. Andrews, J.G. Branson, G.B. Cerati, D. Evans, F. Golf, A. Holzner, R. Kelley, M. Lebourgeois, J. Letts, B. Mangano, S. Padhi, C. Palmer, G. Petrucciani, H. Pi, M. Pieri, R. Ranieri, M. Sani, V. Sharma, S. Simon, E. Sudano, M. Tadel, Y. Tu, A. Vartak, S. Wasserbaech[45], F. Würthwein, A. Yagil, J. Yoo

University of California, Santa Barbara, Santa Barbara, USA
D. Barge, R. Bellan, C. Campagnari, M. D'Alfonso, T. Danielson, K. Flowers, P. Geffert, J. Incandela, C. Justus, P. Kalavase, S.A. Koay, D. Kovalskyi, V. Krutelyov, S. Lowette, N. Mccoll, V. Pavlunin, F. Rebassoo, J. Ribnik, J. Richman, R. Rossin, D. Stuart, W. To, J.R. Vlimant

California Institute of Technology, Pasadena, USA
A. Apresyan, A. Bornheim, J. Bunn, Y. Chen, M. Gataullin, Y. Ma, A. Mott, H.B. Newman, C. Rogan, K. Shin, V. Timciuc, P. Traczyk, J. Veverka, R. Wilkinson, Y. Yang, R.Y. Zhu

Carnegie Mellon University, Pittsburgh, USA
B. Akgun, R. Carroll, T. Ferguson, Y. Iiyama, D.W. Jang, S.Y. Jun, Y.F. Liu, M. Paulini, J. Russ, H. Vogel, I. Vorobiev

University of Colorado at Boulder, Boulder, USA
J.P. Cumalat, M.E. Dinardo, B.R. Drell, C.J. Edelmaier, W.T. Ford, A. Gaz, B. Heyburn, E. Luiggi Lopez, U. Nauenberg, J.G. Smith, K. Stenson, K.A. Ulmer, S.R. Wagner, S.L. Zang

Cornell University, Ithaca, USA
L. Agostino, J. Alexander, D. Cassel, A. Chatterjee, N. Eggert, L.K. Gibbons, B. Heltsley, W. Hopkins, A. Khukhunaishvili, B. Kreis, G. Nicolas Kaufman, J.R. Patterson, D. Puigh, A. Ryd, M. Saelim, E. Salvati, X. Shi, W. Sun, W.D. Teo, J. Thom, J. Thompson, J. Vaughan, Y. Weng, L. Winstrom, P. Wittich

Fairfield University, Fairfield, USA
A. Biselli, G. Cirino, D. Winn

Fermi National Accelerator Laboratory, Batavia, USA
S. Abdullin, M. Albrow, J. Anderson, G. Apollinari, M. Atac, J.A. Bakken, L.A.T. Bauerdick, A. Beretvas, J. Berryhill, P.C. Bhat, I. Bloch, F. Borcherding, K. Burkett, J.N. Butler, V. Chetluru, H.W.K. Cheung, F. Chlebana, S. Cihangir, W. Cooper, D.P. Eartly, V.D. Elvira, S. Esen, I. Fisk, J. Freeman, Y. Gao, E. Gottschalk, D. Green, K. Gunthoti, O. Gutsche, J. Hanlon, R.M. Harris, J. Hirschauer, B. Hooberman, H. Jensen, M. Johnson, U. Joshi, R. Khatiwada, B. Klima, K. Kousouris, S. Kunori, S. Kwan, C. Leonidopoulos, P. Limon, D. Lincoln, R. Lipton, J. Lykken, K. Maeshima, J.M. Marraffino, D. Mason, P. McBride, T. Miao, K. Mishra, S. Mrenna, Y. Musienko[46], C. Newman-Holmes, V. O'Dell, R. Pordes, O. Prokofyev, N. Saoulidou, E. Sexton-Kennedy, S. Sharma, W.J. Spalding, L. Spiegel, P. Tan, L. Taylor, S. Tkaczyk, L. Uplegger, E.W. Vaandering, R. Vidal, J. Whitmore, W. Wu, F. Yang, F. Yumiceva, J.C. Yun

University of Florida, Gainesville, USA
D. Acosta, P. Avery, D. Bourilkov, M. Chen, S. Das, M. De Gruttola, G.P. Di Giovanni, D. Dobur, A. Drozdetskiy, R.D. Field, M. Fisher, Y. Fu, I.K. Furic, J. Gartner, J. Hugon, B. Kim, J. Konigsberg, A. Korytov, A. Kropivnitskaya, T. Kypreos, K. Matchev, G. Mitselmakher, L. Muniz, C. Prescott, R. Remington, A. Rinkevicius, M. Schmitt, B. Scurlock, P. Sellers, N. Skhirtladze, M. Snowball, D. Wang, J. Yelton, M. Zakaria

Florida International University, Miami, USA
V. Gaultney, L. Kramer, L.M. Lebolo, S. Linn, P. Markowitz, G. Martinez, J.L. Rodriguez

Florida State University, Tallahassee, USA
T. Adams, A. Askew, J. Bochenek, J. Chen, B. Diamond, S.V. Gleyzer, J. Haas, S. Hagopian, V. Hagopian, M. Jenkins, K.F. Johnson, H. Prosper, L. Quertenmont, S. Sekmen, V. Veeraraghavan

Florida Institute of Technology, Melbourne, USA
M.M. Baarmand, B. Dorney, S. Guragain, M. Hohlmann, H. Kalakhety, R. Ralich, I. Vodopiyanov

University of Illinois at Chicago (UIC), Chicago, USA
M.R. Adams, I.M. Anghel, L. Apanasevich, Y. Bai, V.E. Bazterra, R.R. Betts, J. Callner, R. Cavanaugh, C. Dragoiu, L. Gauthier, C.E. Gerber, D.J. Hofman, S. Khalatyan, G.J. Kunde[47], F. Lacroix, M. Malek, C. O'Brien, C. Silkworth, C. Silvestre, A. Smoron, D. Strom, N. Varelas

The University of Iowa, Iowa City, USA
U. Akgun, E.A. Albayrak, B. Bilki, W. Clarida, F. Duru, C.K. Lae, E. McCliment, J.-P. Merlo, H. Mermerkaya[48], A. Mestvirishvili, A. Moeller, J. Nachtman, C.R. Newsom, E. Norbeck, J. Olson, Y. Onel, F. Ozok, S. Sen, J. Wetzel, T. Yetkin, K. Yi

Johns Hopkins University, Baltimore, USA
B.A. Barnett, B. Blumenfeld, A. Bonato, C. Eskew, D. Fehling, G. Giurgiu, A.V. Gritsan, Z.J. Guo, G. Hu, P. Maksimovic, S. Rappoccio, M. Swartz, N.V. Tran, A. Whitbeck

The University of Kansas, Lawrence, USA
P. Baringer, A. Bean, G. Benelli, O. Grachov, R.P. Kenny Iii, M. Murray, D. Noonan, S. Sanders, J.S. Wood, V. Zhukova

Kansas State University, Manhattan, USA
A.F. Barfuss, T. Bolton, I. Chakaberia, A. Ivanov, S. Khalil, M. Makouski, Y. Maravin, S. Shrestha, I. Svintradze, Z. Wan

Lawrence Livermore National Laboratory, Livermore, USA
J. Gronberg, D. Lange, D. Wright

University of Maryland, College Park, USA
A. Baden, M. Boutemeur, S.C. Eno, D. Ferencek, J.A. Gomez, N.J. Hadley, R.G. Kellogg, M. Kirn, Y. Lu, A.C. Mignerey, K. Rossato, P. Rumerio, F. Santanastasio, A. Skuja, J. Temple, M.B. Tonjes, S.C. Tonwar, E. Twedt

Massachusetts Institute of Technology, Cambridge, USA
B. Alver, G. Bauer, J. Bendavid, W. Busza, E. Butz, I.A. Cali, M. Chan, V. Dutta, P. Everaerts, G. Gomez Ceballos, M. Goncharov, K.A. Hahn, P. Harris, Y. Kim, M. Klute, Y.-J. Lee, W. Li, C. Loizides, P.D. Luckey, T. Ma, S. Nahn, C. Paus, D. Ralph, C. Roland, G. Roland, M. Rudolph, G.S.F. Stephans, F. Stöckli, K. Sumorok, K. Sung, D. Velicanu, E.A. Wenger, R. Wolf, S. Xie, M. Yang, Y. Yilmaz, A.S. Yoon, M. Zanetti

University of Minnesota, Minneapolis, USA
S.I. Cooper, P. Cushman, B. Dahmes, A. De Benedetti, P.R. Dudero, G. Franzoni, J. Haupt, K. Klapoetke, Y. Kubota, J. Mans, N. Pastika, V. Rekovic, R. Rusack, M. Sasseville, A. Singovsky, N. Tambe

University of Mississippi, University, USA
L.M. Cremaldi, R. Godang, R. Kroeger, L. Perera, R. Rahmat, D.A. Sanders, D. Summers

University of Nebraska-Lincoln, Lincoln, USA
K. Bloom, S. Bose, J. Butt, D.R. Claes, A. Dominguez, M. Eads, J. Keller, T. Kelly, I. Kravchenko, J. Lazo-Flores, H. Malbouisson, S. Malik, G.R. Snow

State University of New York at Buffalo, Buffalo, USA
U. Baur, A. Godshalk, I. Iashvili, S. Jain, A. Kharchilava, A. Kumar, S.P. Shipkowski, K. Smith, J. Zennamo

Northeastern University, Boston, USA
G. Alverson, E. Barberis, D. Baumgartel, O. Boeriu, M. Chasco, S. Reucroft, J. Swain, D. Trocino, D. Wood, J. Zhang

Northwestern University, Evanston, USA
A. Anastassov, A. Kubik, N. Odell, R.A. Ofierzynski, B. Pollack, A. Pozdnyakov, M. Schmitt, S. Stoynev, M. Velasco, S. Won

University of Notre Dame, Notre Dame, USA
L. Antonelli, D. Berry, A. Brinkerhoff, M. Hildreth, C. Jessop, D.J. Karmgard, J. Kolb, T. Kolberg, K. Lannon, W. Luo, S. Lynch, N. Marinelli, D.M. Morse, T. Pearson, R. Ruchti, J. Slaunwhite, N. Valls, M. Wayne, J. Ziegler

The Ohio State University, Columbus, USA
B. Bylsma, L.S. Durkin, J. Gu, C. Hill, P. Killewald, K. Kotov, T.Y. Ling, M. Rodenburg, G. Williams

Princeton University, Princeton, USA
N. Adam, E. Berry, P. Elmer, D. Gerbaudo, V. Halyo, P. Hebda, A. Hunt, J. Jones, E. Laird, D. Lopes Pegna, D. Marlow, T. Medvedeva, M. Mooney, J. Olsen, P. Piroué, X. Quan, B. Safdi, H. Saka, D. Stickland, C. Tully, J.S. Werner, A. Zuranski

University of Puerto Rico, Mayaguez, USA
J.G. Acosta, X.T. Huang, A. Lopez, H. Mendez, S. Oliveros, J.E. Ramirez Vargas, A. Zatserklyaniy

Purdue University, West Lafayette, USA
E. Alagoz, V.E. Barnes, G. Bolla, L. Borrello, D. Bortoletto, M. De Mattia, A. Everett, A.F. Garfinkel, L. Gutay, Z. Hu, M. Jones, O. Koybasi, M. Kress, A.T. Laasanen, N. Leonardo, C. Liu, V. Maroussov, P. Merkel, D.H. Miller, N. Neumeister, I. Shipsey, D. Silvers, A. Svyatkovskiy, H.D. Yoo, J. Zablocki, Y. Zheng

Purdue University Calumet, Hammond, USA
P. Jindal, N. Parashar

Rice University, Houston, USA
C. Boulahouache, K.M. Ecklund, F.J.M. Geurts, B.P. Padley, R. Redjimi, J. Roberts, J. Zabel

University of Rochester, Rochester, USA
B. Betchart, A. Bodek, Y.S. Chung, R. Covarelli, P. de Barbaro, R. Demina, Y. Eshaq, H. Flacher, A. Garcia-Bellido, P. Goldenzweig, Y. Gotra, J. Han, A. Harel, D.C. Miner, D. Orbaker, G. Petrillo, W. Sakumoto, D. Vishnevskiy, M. Zielinski

The Rockefeller University, New York, USA
A. Bhatti, R. Ciesielski, L. Demortier, K. Goulianos, G. Lungu, S. Malik, C. Mesropian

Rutgers, the State University of New Jersey, Piscataway, USA
O. Atramentov, A. Barker, D. Duggan, Y. Gershtein, R. Gray, E. Halkiadakis, D. Hidas, D. Hits, A. Lath, S. Panwalkar, R. Patel, K. Rose, S. Schnetzer, S. Somalwar, R. Stone, S. Thomas

University of Tennessee, Knoxville, USA
G. Cerizza, M. Hollingsworth, S. Spanier, Z.C. Yang, A. York

Texas A&M University, College Station, USA
R. Eusebi, W. Flanagan, J. Gilmore, A. Gurrola, T. Kamon, V. Khotilovich, R. Montalvo, I. Osipenkov, Y. Pakhotin, J. Pivarski, A. Safonov, S. Sengupta, A. Tatarinov, D. Toback, M. Weinberger

Texas Tech University, Lubbock, USA
N. Akchurin, C. Bardak, J. Damgov, C. Jeong, K. Kovitanggoon, S.W. Lee, T. Libeiro, P. Mane, Y. Roh, A. Sill, I. Volobouev, R. Wigmans, E. Yazgan

Vanderbilt University, Nashville, USA
E. Appelt, E. Brownson, D. Engh, C. Florez, W. Gabella, M. Issah, W. Johns, P. Kurt, C. Maguire, A. Melo, P. Sheldon, B. Snook, S. Tuo, J. Velkovska

University of Virginia, Charlottesville, USA
M.W. Arenton, M. Balazs, S. Boutle, B. Cox, B. Francis, R. Hirosky, A. Ledovskoy, C. Lin, C. Neu, R. Yohay

Wayne State University, Detroit, USA
S. Gollapinni, R. Harr, P.E. Karchin, P. Lamichhane, M. Mattson, C. Milstène, A. Sakharov

University of Wisconsin, Madison, USA
M. Anderson, M. Bachtis, J.N. Bellinger, D. Carlsmith, S. Dasu, J. Efron, L. Gray, K.S. Grogg, M. Grothe, R. Hall-Wilton, M. Herndon, A. Hervé, P. Klabbers, J. Klukas, A. Lanaro, C. Lazaridis, J. Leonard, R. Loveless, A. Mohapatra, F. Palmonari, D. Reeder, I. Ross, A. Savin, W.H. Smith, J. Swanson, M. Weinberg

†: Deceased
1: Also at CERN, European Organization for Nuclear Research, Geneva, Switzerland
2: Also at Universidade Federal do ABC, Santo Andre, Brazil
3: Also at Laboratoire Leprince-Ringuet, Ecole Polytechnique, IN2P3-CNRS, Palaiseau, France
4: Also at Suez Canal University, Suez, Egypt
5: Also at British University, Cairo, Egypt
6: Also at Fayoum University, El-Fayoum, Egypt
7: Also at Soltan Institute for Nuclear Studies, Warsaw, Poland
8: Also at Massachusetts Institute of Technology, Cambridge, USA
9: Also at Université de Haute-Alsace, Mulhouse, France
10: Also at Brandenburg University of Technology, Cottbus, Germany
11: Also at Moscow State University, Moscow, Russia
12: Also at Institute of Nuclear Research ATOMKI, Debrecen, Hungary
13: Also at Eötvös Loránd University, Budapest, Hungary
14: Also at Tata Institute of Fundamental Research - HECR, Mumbai, India
15: Also at University of Visva-Bharati, Santiniketan, India
16: Also at Sharif University of Technology, Tehran, Iran
17: Also at Shiraz University, Shiraz, Iran
18: Also at Isfahan University of Technology, Isfahan, Iran
19: Also at Facoltà Ingegneria Università di Roma, Roma, Italy
20: Also at Università della Basilicata, Potenza, Italy
21: Also at Laboratori Nazionali di Legnaro dell' INFN, Legnaro, Italy
22: Also at Università degli studi di Siena, Siena, Italy
23: Also at California Institute of Technology, Pasadena, USA
24: Also at Faculty of Physics of University of Belgrade, Belgrade, Serbia
25: Also at University of California, Los Angeles, Los Angeles, USA
26: Also at University of Florida, Gainesville, USA
27: Also at Université de Genève, Geneva, Switzerland
28: Also at Scuola Normale e Sezione dell' INFN, Pisa, Italy
29: Also at University of Athens, Athens, Greece
30: Also at The University of Kansas, Lawrence, USA
31: Also at Institute for Theoretical and Experimental Physics, Moscow, Russia
32: Also at Paul Scherrer Institut, Villigen, Switzerland
33: Also at University of Belgrade, Faculty of Physics and Vinca Institute of Nuclear Sciences, Belgrade, Serbia
34: Also at Gaziosmanpasa University, Tokat, Turkey
35: Also at Adiyaman University, Adiyaman, Turkey
36: Also at The University of Iowa, Iowa City, USA
37: Also at Mersin University, Mersin, Turkey
38: Also at Izmir Institute of Technology, Izmir, Turkey
39: Also at Kafkas University, Kars, Turkey
40: Also at Suleyman Demirel University, Isparta, Turkey
41: Also at Ege University, Izmir, Turkey
42: Also at Rutherford Appleton Laboratory, Didcot, United Kingdom
43: Also at School of Physics and Astronomy, University of Southampton, Southampton, United Kingdom
44: Also at INFN Sezione di Perugia; Università di Perugia, Perugia, Italy
45: Also at Utah Valley University, Orem, USA
46: Also at Institute for Nuclear Research, Moscow, Russia

47: Also at Los Alamos National Laboratory, Los Alamos, USA
48: Also at Erzincan University, Erzincan, Turkey